

UNIVERSIDADE FEDERAL DE SÃO CARLOS
CENTRO DE CIÊNCIAS EXATAS E DE TECNOLOGIA
DEPARTAMENTO DE ENGENHARIA QUÍMICA

LÚRIMA UANE SOARES FARIA

**ENERGY CONSUMPTION AND REACTION RATE
OPTIMIZATION COMBINING TURBULENCE PROMOTER
AND CURRENT MODULATION FOR ELECTROCHEMICAL
MINERALIZATION**

SÃO CARLOS - SP
2021

LÚRIMA UANE SOARES FARIA

**ENERGY CONSUMPTION AND REACTION RATE OPTIMIZATION COMBINING
TURBULENCE PROMOTER AND CURRENT MODULATION FOR
ELECTROCHEMICAL MINERALIZATION**

Dissertação apresentada ao Programa de Pós-Graduação em Engenharia Química da Universidade Federal de São Carlos, para obtenção do título de mestre em Engenharia Química.

Orientador: Prof. Dr. Luís Augusto Martins Ruotolo

SÃO CARLOS - SP
2021

UNIVERSIDADE FEDERAL DE SÃO CARLOS
Centro de Ciências Exatas e de Tecnologia
Programa de Pós-Graduação em Engenharia Química

Folha de aprovação

Assinatura dos membros da comissão examinadora que avaliou e aprovou a Defesa de Mestrado da candidata Lúrima Uane Soares Faria, realizada em 23/02/2021:

Prof. Dr. Luís Augusto Martins Ruotolo
Universidade Federal de São Carlos

Prof. Dr. José Mário Aquino
Universidade Federal de São Carlos

Prof. Dr. Giancarlo Richard Salazar Banda
Universidade Tiradentes

Prof. Dr. Leonardo Santos Andrade
Universidade Federal de Goiás

ACKNOWLEDGMENTS

I would like to express my gratitude to all those who have helped me or have been an important part of my life during the past years.

First of all, I thank my mother, Maura Gomes de Faria, for her encouragement and care, and my father, Luciano Soares da Silva, for his support and protection, for leaving his own home to accompany me on this journey and make it all possible.

I also thank my brother, Luamós Úride, who is always there when I need him, and my husband, Geanderson Carlos, for his love, support, and encouragement to follow my passions, even with the difficulties and distance.

To all my friends, thanks for the care and encouragement. I am grateful to Camila Rodrigues, Aline Mariana, and Matheus Domingues, for the support, advice, and for always helped me move forward during these years.

To my advisor, Prof. Dr. Luís Augusto M. Ruotolo, for his guidance, dedication, teaching, and the trust and confidence bestowed upon me, as well as to the members of the examining board, Prof. Dr. José Mário Aquino, Prof. Dr. Giancarlo R. S. Banda, and Prof. Dr. Leonardo S. Andrade, for their willingness to contribute to the improvement of this work.

Great gratitude to Prof. Dr. José Mário de Aquino, for all the support and willingness to help, for the teachings, and for the good times shared in the lab. I also thank the professor for the valuable contributions, the questions raised, and the observations pertinent to the work.

To Dr. Alyne B. Veroli, the laboratory technician, as well as to everyone at the Laboratory for Environmental Technologies (LATEA) for their support and companionship.

I am grateful to the Fundação de Amparo à Pesquisa do Estado de São Paulo (FAPESP, grant 2017/19838-5) and Coordenação de Aperfeiçoamento de Pessoal de Nível Superior (CAPES, Finance Code 001) for financial support. I also thank the Conselho Nacional de Desenvolvimento Científico e Tecnológico (CNPq) for the Master fellowship.

SCIENTIFIC PRODUCTION RELATED TO THIS STUDY

The results obtained in this study were published in the indexed journal:

FARIA, L. U.; OLIVEIRA, K. S.; VEROLI, A. B.; AQUINO, J. M.; RUOTOLO, L. A. Energy consumption and reaction rate optimization combining turbulence promoter and current modulation for electrochemical mineralization. **Chemical Engineering Journal**, v. 418, p. 129363, 2021.

RESUMO

No atual cenário mundial, um dos problemas ambientais e de saúde pública que ainda necessita de uma intervenção mais eficiente é a poluição causada por efluentes industriais contendo compostos orgânicos tóxicos, tipicamente tratados por processos biológicos. No entanto, esse método é ineficiente para a degradação de compostos biorefratários, além de gerar uma grande quantidade de lodo e demandar uma maior área física. Em virtude desses fatores, técnicas eletroquímicas têm se destacado como uma alternativa promissora de tratamento, principalmente por sua eficiência e adequação ambiental. Contudo, o consumo energético do processo ainda representa um fator a ser melhorado para sua aplicação efetiva. Nesse sentido, foram abordadas nesse trabalho duas estratégias para superar esse problema. A modulação da corrente é uma delas e consiste no controle da corrente aplicada para que seu valor seja sempre próximo ao da corrente limite do processo. A partir dessa técnica pode-se melhorar a eficiência de mineralização e conseqüentemente reduzir o consumo energético; porém, há o inconveniente de que o tempo de processo torna-se mais longo. Diante disso, a segunda estratégia proposta consistiu no uso de promotores de turbulência (PTs) a fim de elevar a transferência de massa no sistema, contribuindo também com a cinética da reação e assim, diminuir o tempo de eletroxidação. Dessa forma, o acréscimo de tempo devido à aplicação de corrente modulada (CM) pode ser compensado, mantendo a eficiência do processo. Nesse contexto, o objetivo deste trabalho foi otimizar o processo de eletroxidação combinando a modulação da corrente com PTs, a fim de melhorar simultaneamente o consumo energético e o tempo de mineralização. O fenol foi utilizado como molécula modelo neste estudo e sua eletroxidação foi avaliada em um reator eletroquímico de fluxo, utilizando o ânodo de diamante dopado com boro (DDB). Os promotores de turbulência de malha (PTM) plástico e carbono vítreo reticulado (CVR) foram avaliados. A abordagem combinada permitiu a redução do consumo de energia de 168 ± 31 kWh por kg de carbono orgânico total (COT) (modo galvanostático) para 72 ± 6 kWh kg⁻¹ COT (corrente modulada + PTM). Além disso, considerando a remoção de 75% de COT, a utilização dos promotores de turbulência permitiu uma redução do tempo de eletrólise de 420 min para 295 min (~30%) nos processos aplicando-se CM. Sob condições galvanostáticas e regime de controle por transferência de massa, o uso do CVR como promotor de turbulência superou o desempenho da mineralização usando o PTM, devido principalmente à estrutura de sua matriz porosa. Entretanto, a variação do tipo de promotor teve menor influência nas eletrólises sob condições de modulação da corrente, sendo observada uma eficiência semelhante em baixas velocidades de fluxo. Os resultados reforçaram o potencial da eletroxidação para o tratamento de efluentes, abrindo caminho para a obtenção de um processo com rápida cinética de degradação e alta eficiência de mineralização, resultando em baixo consumo de energia.

Palavras-chave: Eletroxidação de orgânicos. Tratamento de efluentes. Controle de transferência de massa. Ânodo de diamante dopado com boro. Eficiência energética.

ABSTRACT

In the current world scenario, one of the environmental and public health problems that still needs a more efficient intervention is the pollution caused by industrial effluents containing toxic organic compounds, typically treated by biological processes. However, this method is inefficient for the degradation of biorefractory compounds, in addition to generating a large amount of sludge and requiring a larger physical area. Due to these factors, electrochemical techniques have stood out as a promising treatment alternative, mainly for their efficiency and environmental compatibility. However, the energy consumption of the process still represents a factor to be improved for its effective application. In this sense, two strategies were approached in this study to overcome this problem. Current modulation is one of them and consists of controlling the applied current so that its value is always close to the limiting value. Using this technique, it is possible to improve the mineralization efficiency and consequently reduce energy consumption; however, there is the drawback that the processing time becomes longer. Considering this, the second proposed strategy consisted of the use of turbulence promoters (TPs) to increase the mass transfer in the system, also contributing to the reaction kinetics and thus, reducing the electrooxidation time. In this way, the time increase due to the application of modulated current (MC) can be compensated, maintaining the efficiency of the process. In this context, this work aimed to optimize the electrooxidation process by combining current modulation with TPs to simultaneously improve energy consumption and mineralization time. Phenol was used as a model molecule in this study and its electrooxidation was evaluated in an electrochemical flow reactor, using the boron-doped diamond anode (BDD). The plastic mesh turbulence promoter (MTP) and reticulated vitreous carbon (RVC) were evaluated. The combined approach enabled the reduction of the energy consumption from 168 ± 31 kWh per kg of total organic carbon (TOC) (galvanostatic mode) to 72 ± 6 kWh kg⁻¹ TOC (modulated current + MTP). Additionally, considering 75% TOC removal, the use of turbulence promoters allowed a reduction in electrolysis time from 420 min to 295 min (~ 30%) in the processes applying MC. Under galvanostatic conditions and mass transfer control regime, the use of RVC as turbulence promoter outperformed the mineralization performance observed using the MTP, mainly due to its porous matrix. However, the variation in the type of promoter had less influence on electrolysis under current modulation conditions, with similar efficiency observed at low flow velocities. The results reinforced the potential of electrooxidation for the treatment of effluents, paving the way for obtaining a process with rapid degradation kinetics and high mineralization efficiency, resulting in low energy consumption.

Keywords: Organics electrooxidation. Wastewater treatment. Mass transfer control. Boron-doped diamond anode. Energy efficiency.

LIST OF FIGURES

| | |
|---|----|
| Fig. 1. (A) Schematic representation of the electrochemical reactor with the mesh turbulence promoter (MTP): 1) BDD anode, 2) flow channel (rubber gasket), 3) mesh turbulence promoter, 4) stainless steel cathode; (B) photograph of the opened reactor with MTP; (C) schematic representation of the electrochemical reactor with the RVC turbulence promoter; and (D) open reactor photograph with RVC. | 33 |
| Fig. 2. (A) Photographs of the turbulence promoters: 1) plastic mesh (MTP), 2) 45 ppi RVC, 3) 60 ppi RVC; and (B) dimensions of the plastic mesh turbulence promoter. | 34 |
| Fig. 3. Schematics of the experimental setup used for the electrolysis: 1) thermostatic bath; 2) heat exchanger; 3) electrolyte reservoir; 4) centrifugal pump; 5) diaphragm valve; 6) rotameter; 7) electrochemical reactor; 8) bypass valve; 9) drain valve; 10) computer; 11) potentiostat; 12) current booster (10 A); 13) differential amplifier; 14) dummy cell; 16) no-break. Oliveira <i>et al.</i> (2020). | 35 |
| Fig. 4. Plots of the normalized phenol (A) and TOC (B) concentrations, as a function of time, for different flow velocities. Electrolysis conditions: $C_{Ph,0} = 130.6 \text{ mg L}^{-1}$ in 0.1 mol L^{-1} Na_2SO_4 ; $\text{TOC}_0 = 100 \text{ mg L}^{-1}$; $i = 30 \text{ mA cm}^{-2}$; $V = 1.4 \text{ L}$. Turbulence promoter: MTP. | 40 |
| Fig. 5. Plots of k_m and $k_{(\text{TOC})}$, as a function of flow velocity. Electrolysis conditions: $C_{Ph,0} = 130.6 \text{ mg L}^{-1}$ in 0.1 mol L^{-1} Na_2SO_4 ; $\text{TOC}_0 = 100 \text{ mg L}^{-1}$; $i = 30 \text{ mA cm}^{-2}$; $V = 1.4 \text{ L}$. Turbulence promoter: MTP. | 41 |
| Fig. 6. Hydroquinone (C_{HQ}) concentrations against time for the electrolysis carried out at different flow velocities using the turbulence promoter MTP. Electrolysis conditions: $C_{Ph,0} = 130.6 \text{ mg L}^{-1}$ in 0.1 mol L^{-1} Na_2SO_4 ; $i = 30 \text{ mA cm}^{-2}$; $V = 1.4 \text{ L}$ | 42 |
| Fig. 7. Catechol (C_{CA}) concentrations against time for the electrolysis carried out at different flow velocities using the turbulence promoter MTP. Electrolysis conditions: $C_{Ph,0} = 130.6 \text{ mg L}^{-1}$ in 0.1 mol L^{-1} Na_2SO_4 ; $i = 30 \text{ mA cm}^{-2}$; $V = 1.4 \text{ L}$ | 43 |
| Fig. 8. (A) Normalized phenol and (B) TOC depletion, according to time, for the electrochemical reactor operating in the absence and presence of different turbulence promoters, using flow velocity (u) of 0.69 m s^{-1} , with $i = 30 \text{ mA cm}^{-2}$. The lines represent the fitted models, according to Eqs. (16) and (21). | 46 |
| Fig. 9. (A) Normalized phenol and (B) TOC depletion, according to time, for the electrochemical reactor operating in the absence and presence of different turbulence promoters, using flow velocity (u) of 0.59 m s^{-1} , with $i = 30 \text{ mA cm}^{-2}$. The lines represent the fitted models, according to Eqs. (16) and (21). | 47 |

Fig. 10. Normalized TOC values, according to time, for the processes carried out using the MC and MC + CC modes, in the absence and presence of different turbulence promoters. Electrolysis conditions: $C_{Ph,0} = 130.6 \text{ mg L}^{-1}$ in $0.1 \text{ mol L}^{-1} \text{ Na}_2\text{SO}_4$; $TOC_0 = 100 \text{ mg L}^{-1}$; $V = 1.4 \text{ L}$; $I_{0app} = 0.48 \text{ A}$ (without TP), $I_{0app} = 0.97 \text{ A}$ (MTP), and $I_{0app} = 1.34 \text{ A}$ (45 ppi RVC).. 50

Fig. 11. Plots of (A) the applied current and (B) the cell potential, according to time, for the processes using CC and MC + CC modes. The charge values correspond to 75% TOC removal.

..... 52

LIST OF TABLES

| | |
|--|----|
| Table 1. Oxidation power of different electrode materials used in the electrooxidation process of organic compounds in acid medium. | 24 |
| Table 2. Semiconductor electrodes commonly used for the electrooxidation of organic compounds..... | 25 |
| Table 3. Values of k_m , δ , and $k_{(TOC)}$ for the processes with turbulence promoter (MTP). | 41 |
| Table 4. Values of k_m , γ , and $k_{(TOC)}$ for the processes carried out using different turbulence promoters and flow velocities..... | 48 |
| Table 5. Values of ε , η , E_{cell} , and t for the processes using CC and MC + CC modes, in the presence and absence of the MTP, considering 75% TOC removal..... | 53 |
| Table 6. Comparison of galvanostatic electrooxidation of phenol under different conditions. | 54 |

LIST OF ABBREVIATIONS

- 3D – Three-dimensional
- AOPs – Advanced oxidation processes
- BDD – Boron-doped diamond
- BOD – Biochemical oxygen demand
- CB – Conduction band
- CC – Constant current
- CECs – Contaminants of emerging concern
- CM – Corrente modulada
- COD – Chemical oxygen demand
- COT – Carbono orgânico total
- CVR – Carbono vítreo reticulado
- DDB – Diamante dopado com boro
- HPLC – High-performance liquid chromatography
- MC – Modulated current
- MTP – Mesh turbulence promoter
- OER – Oxygen evolution reaction
- PTM – Promotor de turbulência de malha
- PTs – Promotores de turbulência
- RVC – Reticulated vitreous carbon
- TOC – Total organic carbon
- TPs – Turbulence promoters
- UV – Ultraviolet light
- VB – Valence band

TABLE OF CONTENTS

| | |
|---|----|
| 1. INTRODUCTION | 12 |
| 2. BIBLIOGRAPHIC REVIEW | 14 |
| 2.1 CONTEXT OF THE STUDY | 14 |
| 2.2 CONVENTIONAL METHODS OF TREATING EFFLUENTS | 15 |
| 2.3 ADVANCED OXIDATIVE PROCESSES (AOPs)..... | 16 |
| 2.3.1 Photocatalytic Processes | 17 |
| 2.3.2 Ozonation | 17 |
| 2.3.3 Fenton Process | 18 |
| 2.3.4 Photo-Fenton Process | 19 |
| 2.4 ELECTROCHEMICAL PROCESSES | 20 |
| 2.4.1 Fundamentals of electrochemical oxidation | 20 |
| 2.4.2 Electrodes for electrochemical oxidation | 23 |
| 2.4.3 Kinetic model for electrochemical degradation of organic compounds and influences of mass and charge transport | 26 |
| 2.4.4 Energy consumption in electrooxidation processes | 29 |
| 3. OBJECTIVES | 31 |
| 4. EXPERIMENTAL | 32 |
| 4.1 CHEMICALS | 32 |
| 4.2 ELECTROCHEMICAL REACTOR, EXPERIMENTAL SETUP, AND ELECTROOXIDATION PROCEDURE | 32 |
| 4.3 LIMITING CURRENT DETERMINATION | 36 |
| 4.4 PERFORMANCE METRICS | 37 |
| 5. RESULTS AND DISCUSSION | 39 |
| 5.1 DETERMINATION OF THE MASS TRANSFER COEFFICIENTS | 39 |
| 5.2 COMPARISON OF THE DIFFERENT TURBULENCE PROMOTERS..... | 44 |
| 5.3 ELECTROOXIDATION COMBINING MODULATED CURRENT AND TURBULENCE PROMOTERS | 48 |
| 6. CONCLUSIONS | 56 |
| 7. SUGGESTIONS FOR FUTURE RESEARCH | 57 |
| REFERENCES | 58 |

1. INTRODUCTION

Pollution of water by contaminants of emerging concern (CECs) has become a major challenge to be resolved worldwide (SEIBERT *et al.*, 2020) due to the potentially deleterious effects of these substances in the aquatic environment and on human health. Among the technologies available to treat water contaminated with CECs, advanced oxidation processes (AOPs) are most attractive, involving the generation of the highly reactive hydroxyl radical ($\bullet\text{OH}$) (MIKLOS *et al.*, 2018). This oxidant can be produced in many ways, but only the electrochemical method can generate it without adding chemicals by water discharge.

In recent decades, electrochemical technology has attracted considerable attention for the treatment of wastewaters containing organic compounds, standing out as one of the most effective ways to remove refractory pollutants (KAPAŁKA *et al.*, 2010). However, despite the advantages of electrooxidation, such as high efficiency, simplicity, easy automation, kinetic control, and versatility, some challenges remain that limit its practical application, especially regarding energy consumption due to low current efficiency, under certain conditions (LIU *et al.*, 2011²).

In galvanostatic electrooxidation, when the applied current (I_{app}) is lower than the limiting current (I_{lim}), the process operates under charge transfer control, with high current efficiency. However, as the concentration decreases, I_{app} surpasses I_{lim} , imposing a mass transfer control and leading to a sharp drop in current efficiency over time, which is translated into high energy consumption. Considering this scenario, an optimized operational condition for the electrooxidation process would be the application of the limiting current throughout the process, consequently minimizing energy consumption (KAPAŁKA *et al.*, 2008). This condition can be achieved by modulating the applied current and maintaining it as close as possible to the limiting value during the electrolysis (PANIZZA *et al.*, 2008).

Electrochemical degradation using modulated current (MC) has been studied for the oxidation of different organic compounds, as reported by Panizza *et al.* (2008), Wang *et al.* (2013), and Urtiaga *et al.* (2014). Oliveira *et al.* (2020) investigated the electrooxidation of a synthetic solution of caffeic acid and real wastewater, applying current modulation to reduce the specific energy consumption. This strategy resulted in ~5-fold lower energy consumption

compared to galvanostatic operation. On the other hand, there was a 1.7-fold increase in the time required for the electrolysis, representing another challenging issue.

It is well known that mass transfer in electrochemical systems can be enhanced using strategies such as increasing the electrolyte flow velocity, promoting turbulence, and gas sparging (ANGLADA *et al.*, 2009). Recently, the use of turbulence promoters (TPs) to enhance mass transfer in electrooxidation processes was shown to be an affordable and efficient way to improve the overall performance of anodic degradation of organics (VEROLI, 2017; WACHTER, 2019). Improved mass transfer can also be achieved using three-dimensional (3D) active anodes, such as PbO₂ films deposited on reticulated vitreous carbon (RVC). Besides providing a greater specific surface area, the porous matrix of these materials promotes hydrodynamic turbulence, consequently increasing the mass transfer rate (FARINOS *et al.*, 2017; FARINOS and RUOTOLO, 2017).

In this study, taking advantage of the use of modulated current and turbulence promoters, a new strategy is presented to optimize both specific energy consumption and operation time for the electrochemical oxidation of organic compounds. This new approach combines the current modulation previously developed by our research group (OLIVEIRA *et al.*, 2020) with turbulence promoters (plastic mesh and reticulated vitreous carbon) to reduce the operational time. Phenol was chosen as a model molecule for proof-of-concept since it is a biorefractory and toxic compound commonly found in many industrial effluents (HARIANI *et al.*, 2015). A boron-doped diamond (BDD) anode was employed in all the experiments.

2. BIBLIOGRAPHIC REVIEW

2.1 CONTEXT OF THE STUDY

The exacerbated consumption of chemicals in different industrial processes leads to the production and release of potentially toxic organic compounds to the environment. Among them, phenolic compounds are considered priority pollutants due to their high toxicity and bioaccumulation, being harmful to organisms even in low concentrations (BRITTO and RANGEL, 2008; YOUSEF *et al.*, 2011; BAZRAFSHAN *et al.*, 2012). According to the World Health Organization (WHO), the maximum permitted limit for phenols in drinking water is 0.001 mg L^{-1} (WHO, 2004).

The presence of these contaminants is common in effluents from various industrial processes. Approximately five million tons of phenolic compounds are produced per year (RIPPEN, 1998; CHASIB, 2013), mainly from pharmaceutical plants, oil refineries, coke plants, pulp, and food processing industries (BRITTO and RANGEL, 2008; PIMENTEL *et al.*, 2008). The concentration of these compounds in wastewater varies for the different industries, such as petrochemicals (3.9 mg L^{-1} to 1230 mg L^{-1}), coke plants (29 mg L^{-1} to 3950 mg L^{-1}), wood products, paints, pharmaceuticals, paper, and cellulose (0.2 mg L^{-1} to 1700 mg L^{-1}), plastic and coal processing (10 mg L^{-1} to 6900 mg L^{-1}), and refineries (5 mg L^{-1} to 600 mg L^{-1}) (CHASIB, 2013).

Phenolic compounds are carcinogenic, mutagenic, and can cause tissue and protein degeneration, and damage to the central nervous system, kidneys, liver, and pancreas in the human body (YOUSEF *et al.*, 2011). Furthermore, they are highly harmful to fauna and flora in aquatic environments. For these reasons, strict laws have been established regarding its concentration in industrial effluents. In Brazil, CONAMA Resolution 430/2011 establishes the maximum allowable content of total phenols in effluents discharged into water bodies of 0.5 mg L^{-1} (BRASIL, 2011). When the release is made in a sewage system, the maximum allowed concentration, in the state of São Paulo, for example, is 5 mg L^{-1} , according to CETESB- Decree N°. 8.468 / 1976.

In this scenario, the importance of reducing the levels of phenolic compounds and other toxic organic substances in wastewater is undeniable, with a constant search for

improvements in the treatment of effluents, which can be done by different methods.

2.2 CONVENTIONAL METHODS OF TREATING EFFLUENTS

The treatment of effluents containing organic compounds can be carried out by traditional physical, chemical, and biological processes or also by AOPs (MARTINEZ-HUITLE *et al.*, 2015), each presenting advantages and disadvantages. The choice of the method to be used depends on different factors, such as efficiency, reliability, ease of control, and operational and installation cost (PANIZZA *et al.*, 2008), with the constant search for more economically viable alternatives that generate less environmental impacts.

The biological process is one of the most used due to its relatively low cost and ability to treat large volumes of effluents (MELO *et al.*, 2009). A classic example of this method is the aerobic system of activated sludge, widely used in the treatment of wastewater with a low concentration of organic matter (KITANOVIĆ and ŠUŠTERŠIČ, 2013). However, biological treatment is inefficient in the degradation of toxic and refractory compounds, such as phenol and its derivatives (KAPAŁKA *et al.*, 2010).

According to Cavalcante (2016), phenols can be biodegraded only when their index is low concerning the Biochemical Oxygen Demand (BOD). Banerjee *et al.* (2010) evaluated the degradation of phenol by two different microorganisms (*Bacillus cereus* MTCC 9817 strain AKG1 and *B. cereus* MTCC 9818 strain AKG2) for various initial concentrations of the pollutant, obtaining, for an initial concentration of 2000 mg L⁻¹, a degradation of only 44.3% and 3.2% for each microorganism studied, in 40 h of process. This result highlights other disadvantages associated with this method, such as the long process time, the need for large operational areas, and the generation of a large volume of sludge (KAPAŁKA *et al.*, 2010).

Concerning physical treatments, the contaminants are not degraded but only transferred or separated to another phase (LIU *et al.*, 2011²). For this reason, these techniques are generally used as pre or post-treatment to remove the dissolved and suspended materials. Physical treatment processes include sedimentation, flotation, filtration, and adsorption (DA SILVA *et al.*, 2015), the latter being one of the most used. Hariani *et al.* (2015) investigated

phenol adsorption at the Ca-bentonite/chitosan composite, concluding that the process was affected by the initial phenol concentration, pH, and contact time. In addition to these operational limitations, other factors such as the need for regeneration of adsorbent materials and low efficiency justify the application of these methods associated with other types of treatment (BAZRAFESHAN *et al.*, 2012; BIGLARI *et al.*, 2017).

The chemical processes are based on the use of reagents, promoting the removal and/or degradation of specific components due to alteration of their chemical structures. Examples of these processes are oxidation and precipitation (GHASEMIAN, 2017). In oxidation, chlorine, chlorine dioxide, hydrogen peroxide, potassium permanganate, among other substances, can be used as oxidants, with chlorine and its derivatives being the most used (KITANOVIĆ and ŠUŠTERŠIČ, 2013). However, chlorination can generate mutagenic and carcinogenic by-products (KETE *et al.*, 2018). Chemical treatments, in most cases, can generate a wide variety of by-products, do not result in complete mineralization of the contaminant, have a low operating capacity, and the need to transport and store reagents (PANIZZA *et al.*, 2008). They are also processes that can have high costs (SALA and GUTIÉRREZ-BOUZÁN, 2012).

Due to the limitations of traditional methods and their low efficiency in treating recalcitrant organic compounds, the search for more innovative and efficient technologies became necessary. In this context, AOPs have stood out as promising alternatives for the treatment of different types of wastewater, with the ability to oxidize a wide variety of organic pollutants (GHASEMIAN, 2017).

2.3 ADVANCED OXIDATIVE PROCESSES (AOPs)

AOPs are characterized by chemical oxidation reactions, mediated mainly by the hydroxyl radical, which can react with contaminants and degrade them to stable inorganic compounds, such as water, carbon dioxide, and salts (CHAICHANAWONG *et al.*, 2010). These processes provide solutions for the treatment of wastewater containing recalcitrant organic compounds, which are difficult to degrade through conventional treatment methods, due to their high chemical stability and/or toxicity to microorganisms, such as dyes, pharmaceuticals, and phenolic products (GHASEMIAN, 2017). Examples of AOPs are

photochemical oxidation, ozonation, UV/H₂O₂, and Fenton reaction (VILLEGAS *et al.*, 2016), in addition to the combination between them (DE MELLO *et al.*, 2018). A brief approach to these methods is presented below.

2.3.1 Photocatalytic Processes

In photocatalytic processes, pollutants are generally degraded under UV radiation in the presence of metal oxide particles, such as ZnO and TiO₂ (EYDIVAND and NIKAZAR, 2015). When a photosensitive substrate is irradiated with appropriate energy ($h\nu$), electrons from the valence band (VB) move to the conduction band (CB), resulting in the photogeneration of electron-hole pairs (e^-/h^+) on the semiconductor surface ($S_{\text{semiconductor}}$) (Eq. 1). The holes (h^+) are neutralized by accepting electrons from water (i.e., hydroxyl ions) to form surface-adsorbed hydroxyl radicals (Eq. 2), which then oxidize the organic pollutants (GHASEMIAN, 2017).



Despite generating good results in the degradation of organic compounds, the efficiency of these methods depends on many parameters, such as the type of photocatalyst used, the type of substrate, its concentration, pH, additives, catalyst load, light intensity, quantity, and type contaminant, among others (BORA and MEWADA, 2017). Ghasemy-Piranloo *et al.* (2019) reported a decrease in the efficiency of phenol degradation when there was an increase in its initial concentration. Furthermore, the use of oxides (e.g., TiO₂) may imply the need to separate it from the solution at the end of the process, which can result in high investment and operating costs (LIU *et al.*, 2011¹).

2.3.2 Ozonation

The use of ozone in chemical oxidation processes is one of the most common methods of treating effluents (BIGLARI *et al.*, 2017). The oxidation of organic and inorganic compounds during ozonation can occur via ozone and/or by hydroxyl radicals produced

according to the reaction shown in Eq. (3).



Ozone reacts slowly with some organic compounds, such as active aromatics, and can produce toxic or even carcinogenic by-products (Wu *et al.*, 2012). Further, the degradation efficiency of this method can be lower than that of other AOPs (BIGLARI *et al.*, 2017). For these reasons, the simultaneous use of ozone with UV radiation and catalysts is preferred, being the simplest and most economical way to accelerate the production rate of hydroxyl radicals to increase the efficiency of the process (Wu *et al.*, 2011). Chaichanawong *et al.* (2010) report an increase in ozonation efficiency from the simultaneous use of ozone with carbon adsorbents. Wu *et al.* (2011) also observed this process optimization through the combination of suction-cavitation and ozonation. Although combinations of ozonation with other AOPs are effective, their industrial application is still limited by their high costs (HSU, 2004).

2.3.3 Fenton Process

In the Fenton process, iron (Fe^{2+}) is used to react with hydrogen peroxide (H_2O_2) and produce hydroxyl radicals (Eq. 4) as the primary reactive product, which will oxidize the target organic pollutant (GHASEMIAN, 2017).



The advantages of this method are simplicity and operational flexibility, easy integration with existing water remediation processes, and relatively low cost compared to other AOPs (CARBAJO *et al.*, 2018). However, the Fenton reaction is affected by different operational parameters, such as the concentration and ratio between the reagents (H_2O_2 and Fe^{2+}), solution pH, time, temperature, and pollutant concentration (BELLO *et al.*, 2019); the most critical factors being the pH and concentration of the reagents.

The excess of any of the reagents, for example, can lead to the elimination of the

hydroxyl radical, forming less reactive species and consequently reducing the performance of the process (MUANGTHAI *et al.*, 2010). Regarding pH, the main disadvantage is that the Fenton reaction is effective only in acidic conditions, while most wastewater has pH values ranging from 5 to 7 (LAM and HU, 2007). To circumvent this problem, some authors suggest the use of other transition metals. Inchaurredo *et al.* (2014), for example, studied the use of copper in conjunction with the Fenton process to obtain complete oxidation of phenol more efficiently.

2.3.4 Photo-Fenton Process

The Photo-Fenton process, a combination of UV with the Fenton reaction, is a more efficient and less pH-dependent treatment method than the typical Fenton process (ATHARIZADE and MIRANZADEH, 2015). The irradiation leads to the photoreduction of Fe^{3+} to Fe^{2+} , which produce new $\bullet OH$ with H_2O_2 (Eq. 4) or according to the following mechanism (Eq. 5):



Therefore, the higher oxidation efficiency is due to the regeneration of Fe^{2+} and the production of additional hydroxyl radicals (AYOUB *et al.*, 2018). According to Hadjltaief *et al.* (2015), an important factor to be observed in these processes is the wavelength. The authors obtained complete degradation of phenol in less time when using UV-C ($\lambda = 254$ nm) compared to the process with UV-A ($\lambda = 365$ nm). However, the limitations concerning the application conditions and the high cost are still factors to be overcome in these processes (PIMENTEL *et al.*, 2008).

In general, among the advantages of AOPs can be cited its high degradation capacity of organic pollutants, not generating excess solid waste as in conventional processes, and faster reaction rates (BIGLARI *et al.*, 2016). However, although highly efficient, these techniques have some drawbacks when considering their industrial application, such as high energy consumption and/or expensive or unstable chemical reagents, and the fact that they are often unable to remove all recalcitrant compounds, forming intermediates non-

biodegradable (MARTINEZ-HUITLE *et al.*, 2015). Therefore, it became necessary to search for new technologies that are environmentally friendly and more efficient in the degradation of recalcitrant organic matter.

In this context, electrochemical processes have been studied as an alternative to traditional methods due to advantages such as high efficiency, ease of operation, and environmental compatibility (LIU *et al.*, 2011²), since they can lead to the mineralization of organic compounds in the solution, without the use of chemical additives, as often observed in AOPs (DE MELLO *et al.*, 2018).

2.4 ELECTROCHEMICAL PROCESSES

Electrooxidation has stood out as one of the most promising alternatives for the treatment of effluents containing non-biodegradable pollutants (KAPAŁKA *et al.*, 2010). The effectiveness of this method was tested with a wide variety of effluents, with potential application for the treatment of landfill leachate, dyes, effluents with high salinity, and herbicides, among other toxic organic compounds (DOMINGUEZ-RAMOS and IRABIEN, 2013).

Despite its advantages, such as environmental friendliness, high efficiency, and simplicity, some factors still represent a limitation of its industrial application, for example, the high energy consumption under certain conditions. Thus, the study of different electrodes and reactions involved in electrochemical degradation and their integration with knowledge about the reactor configuration and hydrodynamics are necessary and may contribute to the optimization of this treatment and its effective application on a large scale (MARTÍNEZ-HUITLE and PANIZZA, 2018).

2.4.1 Fundamentals of electrochemical oxidation

Electrochemical oxidation of organic components can be classified into direct and indirect oxidation. In direct oxidation, electron transfer occurs on the electrode surface, without the participation of other substances; on the other hand, in indirect oxidation, organic

pollutants are oxidized through the mediation of some electroactive species generated on the anode surface, which act as intermediates for the transfer of electrons between the electrode and organic compounds (MARTÍNEZ-HUITLE and PANIZZA, 2018).

Direct electrolysis requires the adsorption of pollutants on the electrode and can occur at relatively low potentials. The process takes place in two stages: diffusion of organic compounds (R) from the bulk solution to the anode surface, in which it is adsorbed; and oxidation of pollutants on the electrode surface, from the direct transfer of electrons to the anode, as expressed in Eq. 6 (ANGLADA *et al.*, 2009). Direct oxidation rates can be affected by diffusion limitations, slow reaction kinetics, and a decrease in the electrode's catalytic activity in the presence of dissolved solutes (poisoning) (COMNINELLIS and CHEN, 2010); besides also depending on the current density. Therefore, the efficiency of the electrochemical process will depend on the relationship between the mass transfer of the substrate and the electron transfer on the electrode surface. This type of oxidation is prevalent on the surface of anodes with high electrocatalytic activity, but which generally present low degradation efficiencies (ANGLADA *et al.*, 2009).



According to Anglada *et al.* (2009), during the anodic oxidation of organic pollutants, two different pathways can be followed: i) electrochemical conversion, in which organic compounds are only partially oxidized (can form biodegradable ones) and they generally require subsequent treatment (Eq. 7) and ii) electrochemical combustion, in which organic compounds are completely mineralized in water, carbon dioxide and other inorganic components (Eq. 8).

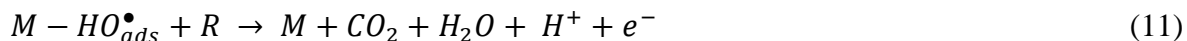


Both approaches require the application of high anode potentials, thus causing

competition with the oxygen evolution reaction (OER). On the other hand, direct oxidation is theoretically possible with low potential values (before the OER), as stated earlier, but the reaction rate is generally slow and strongly dependent on the electrocatalytic activity of the anode. The OER (Eq. 9) can occur competitively in aqueous electrolytes in most anodic processes, which is an undesirable parallel reaction since it consumes the hydroxyl radicals produced, reducing the efficiency of the process (GHASEMIAN, 2017).



Regarding indirect oxidation, it is mediated by electrogenerated chemical species. The most common species is the hydroxyl radical, formed from water discharge on the anode surface (Eq. 10). When hydroxyl radicals are physically adsorbed on "non-active" electrodes, they can lead to total pollutant mineralization (Eq. 11). If adsorption occurs chemically on a metal oxide (MO) anode, an "active" electrode, there will be the formation of higher oxidation states available on the electrode surface (M), which will result in partial degradation of organic compounds (Eq. 12 and 13) (GHASEMIAN, 2017).



The formation of other oxidizing species depends on the electrocatalytic activity of the anode (MARTÍNEZ-HUITLE *et al.*, 2015) and the most common oxidants that can be produced electrochemically are chlorine (Cl₂), hydrogen peroxide (H₂O₂), peroxydisulfuric acid (H₂S₂O₈), and ozone (O₃). Metallic catalytic mediators (such as Ag²⁺, Co³⁺, Fe³⁺) are also used to generate hydroxyl radicals, as in the electro-Fenton process. However, the use of metal ions can result in an effluent that is more toxic than the initial one, requiring an

additional treatment step to remove them (ANGLADA *et al.*, 2009).

The oxidation of organic pollutants occurs in the region of OER potentials and determines the selectivity and efficiency of the treatment, and this characteristic depends heavily on the anode used and will determine its capacity to produce hydroxyl radicals (MARTÍNEZ-HUITLE *et al.*, 2015). The selection of the process will therefore depend not only on the experimental conditions and composition of the electrolyte but also, and especially, on the nature and structure of the electrode material.

2.4.2 Electrodes for electrochemical oxidation

The electrode material is one of the major determinants of the efficiency of electrochemical treatment, as well as the potential for the formation of toxic by-products. These materials should have characteristics such as high stability (physical and chemical); catalytic activity and selectivity; resistance to corrosion, erosion, and passivation; high electrical conductivity; and low cost/life ratio (ANGLADA *et al.*, 2009).

One of the factors to be considered to assess the selectivity of the electrode material is the competition between the oxidation reaction of organic compounds with the parallel reaction of oxygen evolution. According to this concept, Comninellis (1994) classified the anodes into active and non-active, according to the interaction of hydroxyl radicals generated with the electrode surface. In the active anodes, for example, IrO₂, RuO₂, and Pt, this interaction is strong, the level of overpotential for the OER is low; consequently, they exhibit a low capacity to transform recalcitrant organic compounds. On the other hand, non-active anodes, such as PbO₂, SnO₂, and BDD, exhibit greater overpotential for OER, with weak interaction between hydroxyl radicals and the electrode surface and, therefore, have greater efficiency in the oxidation of recalcitrant organic compounds. Thus, the weaker this interaction, the lower the electrochemical activity towards the oxygen evolution reaction and the greater the chemical reactivity concerning organic oxidation. Based on this approach, different anode materials were classified by Kapalka *et al.* (2008) according to their oxidation power in acidic media, as shown in Table 1.

Table 1. Oxidation power of different electrode materials used in the electrooxidation process of organic compounds in acid medium.

| Electrode | Oxidation potential (V) | Overpotential for OER (V) | Adsorption enthalpy of •OH | Oxidation power of the anode |
|---|-------------------------|---------------------------|----------------------------|------------------------------|
| RuO ₂ -TiO ₂ (DSA-Cl ₂) | 1.4 – 1.7 | 0.18 | Chemisorption | Lower |
| IrO ₂ -Ta ₂ O ₅ (DSA-O ₂) | 1.5 – 1.8 | 0.25 | ↑ | ↓ |
| Ti-Pt | 1.7 – 1.9 | 0.3 | | |
| Ti/PbO ₂ | 1.8 – 2.0 | 0.5 | | |
| Ti/SnO ₂ -Sb ₂ O ₃ | 1.9 – 2.2 | 0.7 | | |
| p-Si/BDD | 2.2 – 2.6 | 1.3 | Physisorption | Higher |

*DSA: Dimensionally stable anodes. Adapted from Kapalka *et al.* (2008).

It is observed in Table 1 that BDD anodes can present higher oxidation rates and greater efficiency than other commonly used materials, such as PbO₂ and Ti/SnO₂-Sb₂O₃. This fact is because they generate a greater amount of •OH poorly adsorbed on the electrode surface (Eq. 14), which implies faster oxidation of pollutants (RADJENOVIC and SEDLAK, 2015).



BDD electrodes have other advantages such as an inert surface, good corrosion stability, a wide potential window in aqueous media (PANIZZA and CERISOLA, 2005), and long life, being promising anodes for the treatment of wastewater on an industrial scale. Many synthetic and real effluents have been completely mineralized with high efficiency using BDD anodes, up to 100% (MARTÍNEZ-HUITLE and PANIZZA, 2018). Kornienko *et al.* (2011), for example, reports high degrees of phenol mineralization of up to 99.7%.

Weiss *et al.* (2008) compared the performance of two electrode materials, PbO₂ and BDD, for phenol degradation. Under charge transfer control, the removal of phenol and the

reduction of Total Organic Carbon (TOC) and Chemical Oxygen Demand (COD) was faster and more effective with the BDD electrode than with the PbO₂ electrode. In addition, the number and quantity of intermediates were higher with PbO₂. They also analyzed the energy consumption for both processes, obtaining a 99% removal of aromatic compounds in about 5 h with the BDD anode, consuming 80 kWh m⁻³ of energy. While the same reduction was achieved with a PbO₂ anode, but for 330 kWh m⁻³ of energy consumption. Therefore, the authors concluded that BDD's electrocatalytic activity was the best. These results also confirm that, despite its high cost, the use of the BDD electrode may be feasible.

Li *et al.* (2005) compared the phenol electrooxidation process using Ti/SnO₂-Sb, Ti/RuO₂, and Pt anodes. The best result was obtained with the Ti/SnO₂-Sb anode, followed by Pt and Ti/RuO₂, in that order. The phenol was quickly oxidized by the Ti/SnO₂-Sb anode, obtaining complete degradation after 5 h of electrolysis; this time was extended to about 18 h for the Pt anode and 36 h for Ti/RuO₂. In addition to longer degradation times related to these anodes, oxide electrodes have a short useful life compared to BDD electrodes (FENG *et al.*, 2016). Other advantages and disadvantages of different types of electrodes are summarized in Table 2.

Table 2. Semiconductor electrodes commonly used for the electrooxidation of organic compounds.

| Semiconductor electrode | Advantages | Drawbacks |
|-------------------------|---|--|
| BDD | <ul style="list-style-type: none"> - Wide potential window - Inert surface - Low adsorption - Corrosion stability - Low double-layer capacitance | <ul style="list-style-type: none"> - High cost |
| PbO ₂ | <ul style="list-style-type: none"> - Inexpensive - Easy to prepare - Good conductivity - Chemical stability - High overpotential for OER | <ul style="list-style-type: none"> - Lower degradation efficiency compared to BDD |
| SnO ₂ -Sb | <ul style="list-style-type: none"> - Rapid oxidation kinetics - Good conductivity - High overpotential for OER | <ul style="list-style-type: none"> - Deactivation |

Adapted from Ghasemian (2017).

Due to their unique characteristics, BDD electrodes are being extensively studied and used in several applications, especially in the treatment of effluents containing organic and/or inorganic pollutants, since their high potential for OER allows the production of hydroxyl radicals with great current efficiency. These radicals are also strong oxidizing agents, very reactive, and with low selectivity, characterizing electrochemistry as a good alternative to the common AOPs (WÄCHTER, 2014).

2.4.3 Kinetic model for electrochemical degradation of organic compounds and influences of mass and charge transport

A kinetic model to describe the electrochemical mineralization of organic pollutants in an aqueous medium, using BDD electrode, was developed by Kapalka *et al.* (2008), considering the hydroxyl radicals electrogenerated and poorly adsorbed on the anode surface as the primary reactants of the oxidation of the compounds.

The following assumptions were made to simplify the model: 1) the adsorption of molecules on the electrode surface can be neglected; 2) all organic species have the same diffusion coefficient; and 3) the rate of the reaction between organic compounds and hydroxyl radicals is very fast and controlled by the mass transport of these substances to the electrode surface, being independent, therefore, of the nature of the pollutant. From these hypotheses, the limiting current of the system, which expresses the current in which the rate of the oxidation process is totally limited by mass transport, can be defined by Eq. 15 as:

$$I_{lim}(t) = n F k_m A C_{Ph}(t) \quad (15)$$

Where $I_{lim}(t)$ is the limiting current (A) at a given time t (s), n the number of electrons involved in the reaction, F the Faraday constant ($A \text{ s mol}^{-1}$), k_m the mass transfer coefficient (m s^{-1}), A the electrode geometric area (m^2), and $C_{Ph}(t)$ the concentration of organic species (mol m^{-3}) in time t (s) of electrolysis.

From Eq. 15 and according to the applied current density (i_{app}) in a galvanostatic process, it is possible to identify two different operational regimes: 1) $i_{apl} < i_{lim}$ for processes under charge transfer control and 2) $i_{app} > i_{lim}$ for mass transfer controlled processes.

In the first case, the current efficiency is high, reaching 100%, since all the charge

supplied is used for the electrogeneration of oxidizing species, which in turn, will immediately react with the organic molecules. In the second case, when the applied current becomes greater than the limiting current and the reaction is controlled by mass transport, parallel reactions, such as OER, begin to occur, causing a gradual decrease in current efficiency over time. When the applied current equals the limiting current for a given concentration, the process operates under optimized kinetics and current efficiency conditions, thus resulting in an optimized condition of energy consumption.

By controlling the current applied in the limiting current condition, it is possible to optimize the process in terms of reducing efficiency losses, as proposed by Panizza *et al.* (2008), through the modulation of the applied current for processes controlled by mass transport. This technique is based on the control of the applied current so that its value is kept as close as possible to the limiting current.

The modulated current has been studied for the electrooxidation of organic compounds by different authors such as Panizza *et al.* (2008), Wang *et al.* (2013), and Oliveira *et al.* (2020), using 3,4,5-trihydroxybenzoic acid, thiophene-2,5-dicarboxylic acid, and caffeic acid as the model molecule, respectively. This same technique was also applied for the electrochemical removal of metal ions from aqueous solutions by Britto-Costa and Ruotolo (2011), who evaluated the copper electrodeposition process. In the case of electrooxidation of organic compounds, the authors confirmed the reduction of energy consumption and greater efficiency using the current modulation technique; however, it is important to note that an increase in process time was identified.

The effects of flow and current on electrochemical oxidation are directly linked to the above-mentioned mass and charge transfer control regimes. When the process is controlled by mass transport, the fluid dynamic turbulence condition favors the transport of species from the bulk to the electrode surface, bringing an improvement in the mass transport coefficient and, consequently, in the kinetics and current efficiency. For the same flow, the increase in current may lead to the occurrence of competitive reactions, such as OER. On the other hand, when the process is under the control of charge transfer, the process kinetics is not affected by fluid dynamic conditions, and the increase in the applied current results in greater removal of the organic compound, which may decrease the treatment time (COMNINELLIS *et al.* 2008; MARTÍNEZ-HUITLE *et al.*, 2015).

To improve mass transport in these processes, some techniques can be used, such as increasing the electrolyte flow rate, using deflectors or turbulence promoters, and gas sparging (ANGLADA *et al.*, 2009). Regarding the turbulence promoters, these can be of different materials, such as carbon fiber and other fabrics, polymeric meshes, expanded metallic or semiconductor structures (three-dimensional electrodes), among others. In general, the shape and orientation of the mesh concerning the electrolyte flow will guarantee an effective improvement in the supply of species to the electrode surface (RAGNINI, 2001).

Veroli (2017) studied the influence of a TP on the electrooxidation of paracetamol and observed a significant improvement in the degradation kinetics of the compound for different flows. In addition to decreasing the operation time, less average energy consumption and electrical load were observed, as well as an increase in current efficiency. For example, using a paracetamol solution with an initial TOC concentration of 100 mg L^{-1} in $0.1 \text{ mol L}^{-1} \text{ Na}_2\text{SO}_4$ at a flow rate of 6 L min^{-1} , the values obtained for kinetic constant and energy consumption for 80% TOC removal were: 0.0118 min^{-1} and $365.13 \text{ kWh kg}^{-1} \text{ TOC}$, respectively. Using TP at the same flow rate, the values obtained from these same parameters were 0.0295 min^{-1} and $209.1 \text{ kWh kg}^{-1} \text{ TOC}$, respectively. Similar conclusions were discussed by Wachter (2019) for the degradation of bisphenol S, whose results showed that the use of a turbulence promoter of three overlapping meshes led to approximately a triplication of the mass transfer coefficient compared to the process without a promoter.

Farinos *et al.* (2017) and Farinos and Ruotolo (2017) also improved mass transport by using a three-dimensional electrode of PbO_2 electrodeposited on 45 and 60 ppi RVC, respectively, for discoloration of the Reactive Blue 19 dye and electrooxidation of the glyphosate herbicide. In this case, the authors observed that, in addition to providing a greater specific surface area, the porous matrix also contributed to greater hydrodynamic turbulence and, consequently, an increase in the mass transfer rate. Reticulated vitreous carbon has been widely used in electrochemical processes due to its large specific surface area, but also for characteristics such as low resistance to fluid flow, high electrical conductivity, low density, and high resistance to corrosion (VASCONCELOS *et al.*, 2019).

Given the presented aspects, it is clear the importance of the operating conditions and the reactor configuration (LIU *et al.*, 2011²) for the optimization of electrochemical processes, considering that some of the main parameters that determine its performance are:

the potential of the electrode, the current densities, mass transport, and electrode materials (MARTÍNEZ-HUITLE and ANDRADE, 2011). Thus, from the study of these parameters, it is possible to obtain the mineralization of organic compounds with greater efficiency and less energy consumption.

2.4.4 Energy consumption in electrooxidation processes

In the electrochemical oxidation of organic compounds, the technical viability of the process is commonly evaluated in terms of the rate of pollutant degradation, while the economic viability is determined by the specific energy consumption (ANGLADA *et al.*, 2009). There are different quantitative parameters used to evaluate the performance of an electrochemical reactor, with emphasis on current efficiency (ε) and energy consumption (η). Current efficiency is associated with both the selectivity of the reaction and the effectiveness of the process, which can be correlated with operating and capital costs. It indicates how much of the charge supplied to the process was actually used for the degradation of organic compounds. Concerning energy consumption, it expresses the amount of energy consumed in the process to mineralize a unit of mass of the organic molecule and is directly related to operating costs (FARINOS, 2016).

Calculations of energy consumption can be useful to estimate costs and to decide which is the best working current density for a specific electrode material (PELEGRINO *et al.*, 2002). It is worth mentioning that the specific energy consumption depends on several factors, such as the reactor design (distance between electrodes, for example), operational parameters (such as electrode potential and current, electrolyte flow), and electrolyte characteristics (conductivity and presence of chloride) (RADJENOVIC and SEDLAK, 2015).

Several authors have confirmed that the efficiency of instantaneous current remains at values close to 100% when electrolysis with BDD anode is performed under the conditions of charge transfer control and decreases when the electrochemical process is under control of mass transport. However, applying current density values well below the limiting current density leads to electrode deactivation, the electrochemical cell will be underutilized, and, as a result, the oxidation kinetics will be slow. The resulting increase in investment costs related to the purchase of a larger number of cells would probably hinder the industrial

implementation of the process (URTIAGA *et al.*, 2014).

In this context, Oliveira *et al.* (2020) report higher mineralization efficiency values for the process using modulated current than for the galvanostatic process for the degradation of caffeic acid. The authors relate these data to the fact that parallel reactions such as OER can be avoided by using current modulation. Also, the values of specific energy consumption were much lower for the process carried out under modulated current conditions. With the application of a constant current in electrooxidation processes, the energy consumption was estimated by the authors at 28.3-30.7 kWh m⁻³, which corresponds to 4.0-4.3 US\$/m³ of treated effluent. On the other hand, the modulated process would require energy consumption of 4.6-5.7 kWh m⁻³, reducing the cost to 0.6-0.8 US\$/m³, making it more attractive economically. Thus, MC is shown to be a promising technique, despite leading to high degradation times, which can be improved by increasing the mass transfer in the system.

3. OBJECTIVES

This study aims to optimize the electrooxidation process of organic compounds from the application of modulated current and the use of turbulence promoters. Specific objectives include:

- Investigate the performance of the phenol electrooxidation process in an electrochemical flow reactor, in the absence and presence of turbulence promoters and identify some possible reactive intermediates;
- Compare the different turbulence promoters (MTP and RVC) and evaluate the influence of their layout on processes under constant current and modulated current;
- Study the process through the control of the applied current, modulated current, and compare with the galvanostatic process, for systems with and without turbulence promoter;
- Evaluate the effect of the combination of modulated current and turbulence promoters on mineralization efficiency, energy consumption, and operational cost of the electrooxidation process.

4. EXPERIMENTAL

4.1 CHEMICALS

Phenol (99%, Sigma-Aldrich) and sodium sulfate (99%, Synth) were used to prepare the electrolyte. Benzoquinone (99%, Acros), hydroquinone (99%, Acros), catechol (99%, Acros), potassium phosphate monobasic (99%, Sigma-Aldrich), and methanol (99.9%, Tedia) were used in the high-performance liquid chromatography (HPLC) analysis. For the TOC analysis, phosphoric acid (85%, Panreac) and sodium persulfate ($\geq 98\%$, Sigma-Aldrich) were employed. All solutions were prepared with deionized water (Millipore Milli-Q system, $\rho \geq 18.2 \text{ M}\Omega \text{ cm}$).

4.2 ELECTROCHEMICAL REACTOR, EXPERIMENTAL SETUP, AND ELECTROOXIDATION PROCEDURE

The electrochemical reactor used in the electrooxidations is shown in Fig. 1. It was composed of two juxtaposed acrylic plates, with a BDD anode ($4.0 \text{ cm} \times 7.0 \text{ cm}$) on one side and a stainless steel AISI 316 cathode ($4.0 \text{ cm} \times 7.0 \text{ cm}$) on the other side, separated by a 3 mm rubber gasket that provided the flow channel (cross-sectional area = 1.2 cm^2) and sealing. The BDD anode was purchased from EUT GmbH (Germany). The diamond layer with 4500 ppm boron doping was $5 \mu\text{m}$ thick, with $\pm 10\%$ homogeneity, deposited on a 2.0 mm niobium substrate.

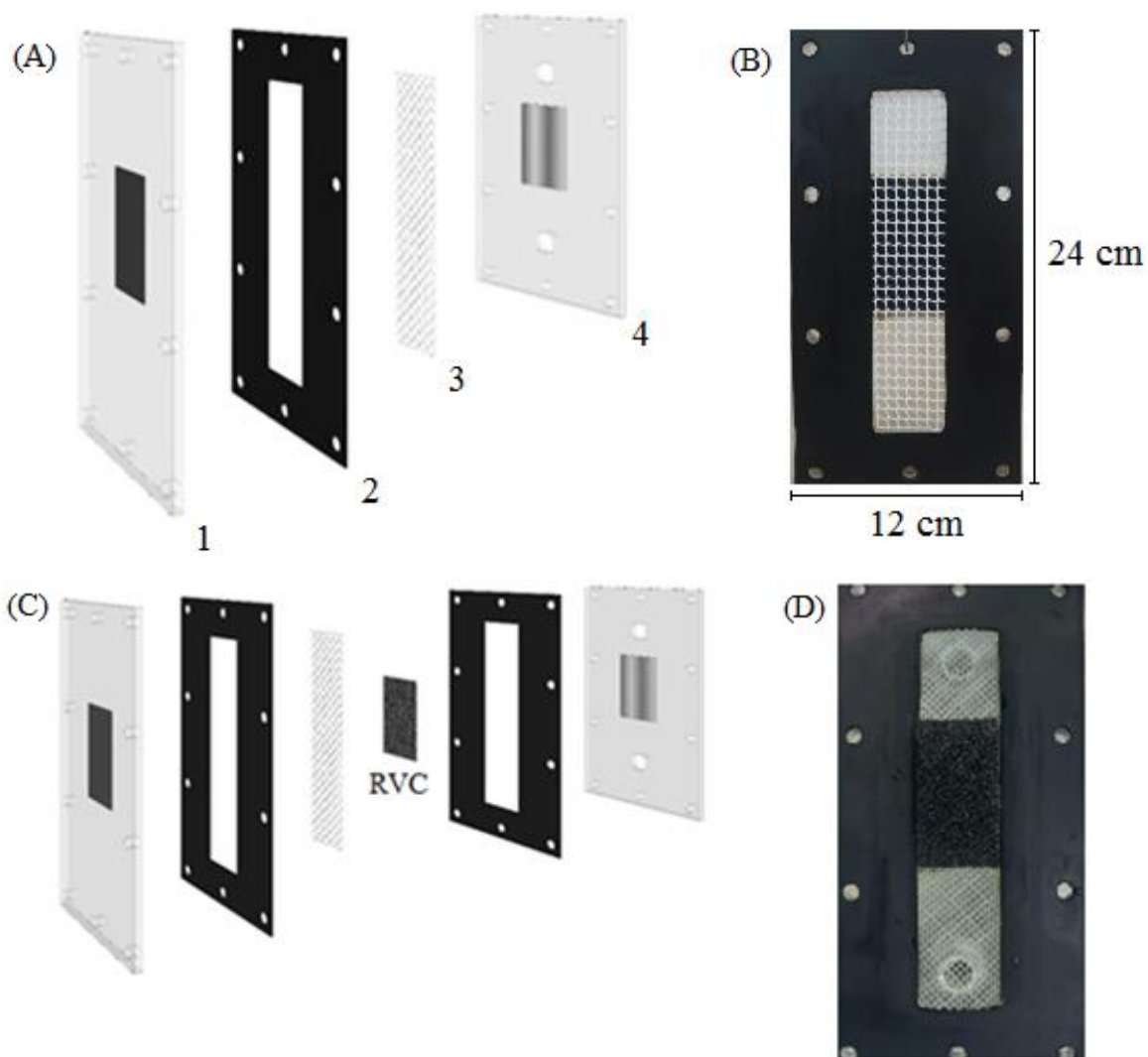


Fig. 1. (A) Schematic representation of the electrochemical reactor with the mesh turbulence promoter (MTP): 1) BDD anode, 2) flow channel (rubber gasket), 3) mesh turbulence promoter, 4) stainless steel cathode; (B) photograph of the opened reactor with MTP; (C) schematic representation of the electrochemical reactor with the RVC turbulence promoter; and (D) open reactor photograph with RVC.

In the experiments using turbulence promoters, a plastic mesh ($1.0 \text{ mm} \times 4.0 \text{ cm} \times 18 \text{ cm}$) or reticulated vitreous carbon (2.5 mm or 5.0 mm thickness $\times 4.0 \text{ cm} \times 7.0 \text{ cm}$) were placed in the flow channel of the electrochemical cell, as shown in Figs. 1 (A and B) and (C and D), respectively. The promoters used and the dimensions of the plastic mesh are shown in detail in Fig. 2. In the case of the RVC (purchased from ERG Co., USA), two different porosities of 45 and 60 ppi (pores per inch) were evaluated. The performance of each

turbulence promoter was analyzed in terms of the mass transfer enhancement factor ($\gamma = k_{m, \text{with promoter}} / k_{m, \text{without promoter}}$).

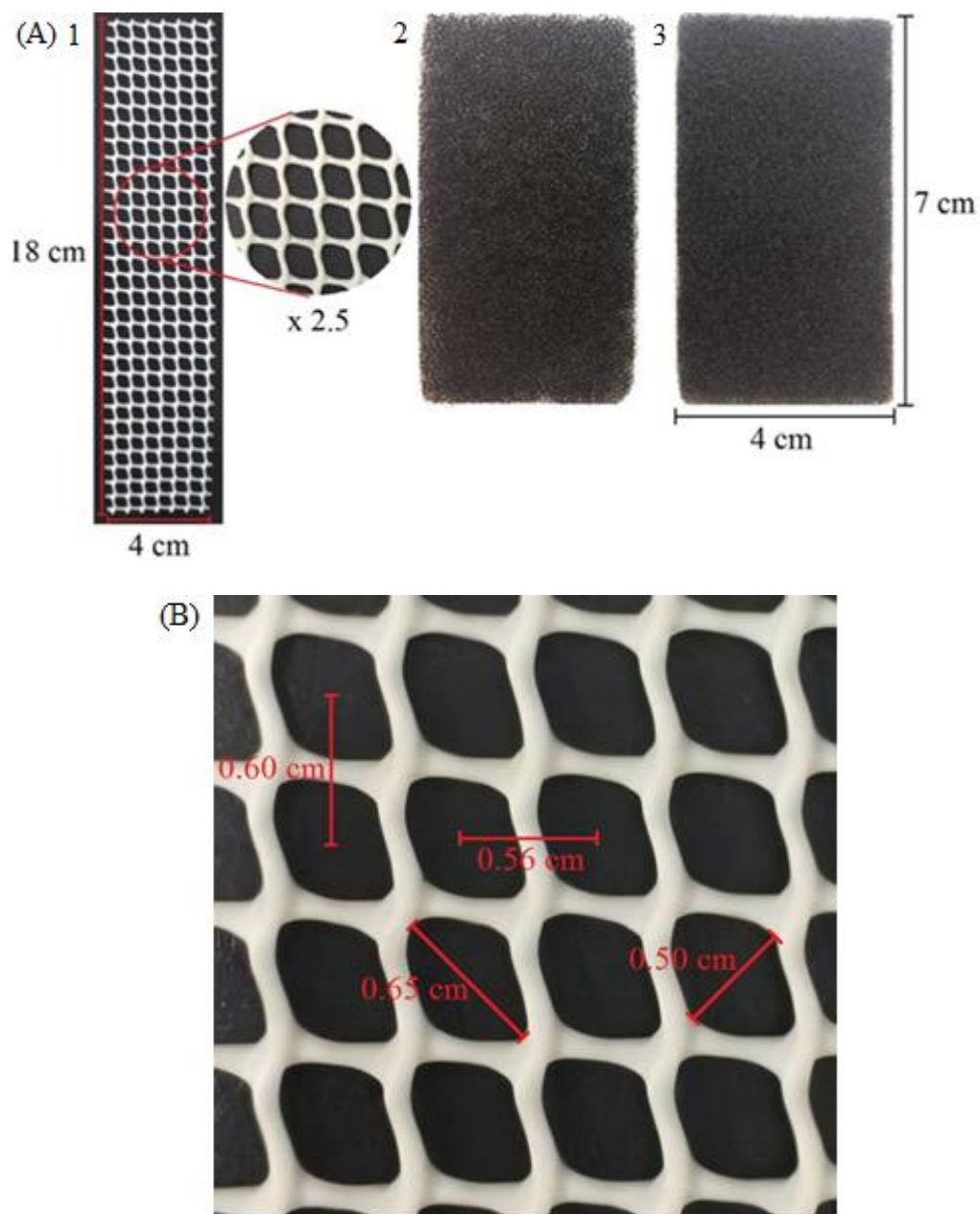


Fig. 2. (A) Photographs of the turbulence promoters: 1) plastic mesh (MTP), 2) 45 ppi RVC, 3) 60 ppi RVC; and (B) dimensions of the plastic mesh turbulence promoter.

The electrooxidation of phenol was carried out using the same experimental setup

employed by Oliveira *et al.* (2020), shown in Fig. 3.

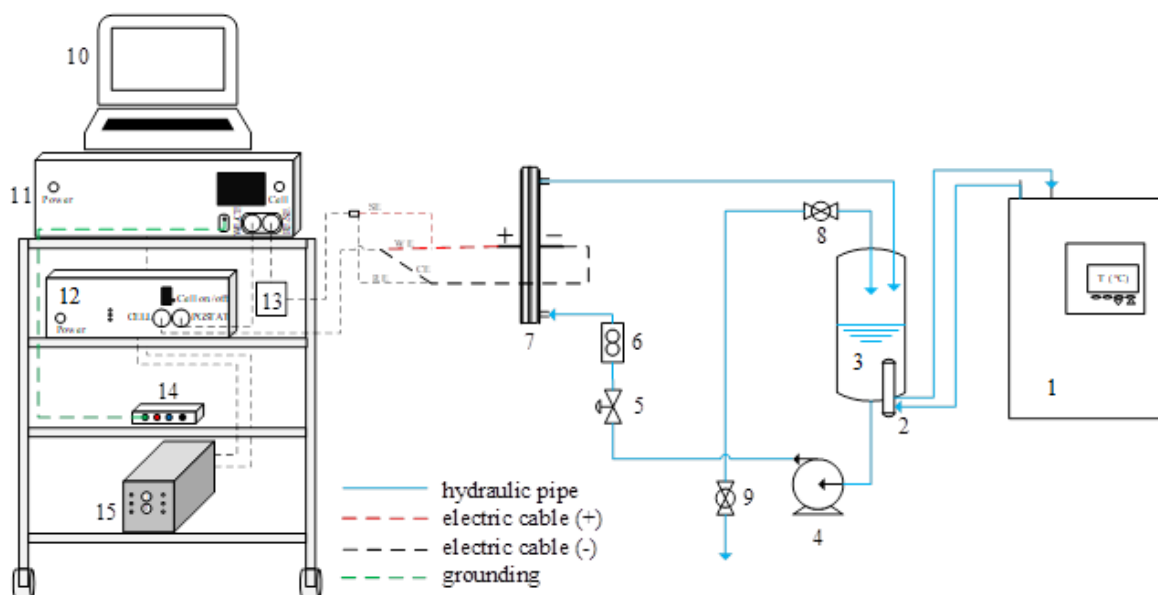


Fig. 3. Schematics of the experimental setup used for the electrolysis: 1) thermostatic bath; 2) heat exchanger; 3) electrolyte reservoir; 4) centrifugal pump; 5) diaphragm valve; 6) rotameter; 7) electrochemical reactor; 8) bypass valve; 9) drain valve; 10) computer; 11) potentiostat; 12) current booster (10 A); 13) differential amplifier; 14) dummy cell; 16) no-break. Oliveira *et al.* (2020).

Before starting each experiment, the BDD electrode was submitted to an anodic pretreatment at 30 mA cm^{-2} for 20 min, in $0.1 \text{ mol L}^{-1} \text{ Na}_2\text{SO}_4$, to clean the surface and remove adsorbed impurities (WACHTER, 2019). The supporting electrolyte (1.4 L) was $0.1 \text{ mol L}^{-1} \text{ Na}_2\text{SO}_4$ containing 130.6 mg L^{-1} phenol, equivalent to $100 \text{ mg L}^{-1} \text{ TOC}$.

The electrooxidation was carried out in constant current (CC) or modulated current modes, using a constant current source (MPC-3006D, Minipa) or a potentiostat (PGSTAT30, Autolab), respectively. Electrolysis combining the modes (MC + CC) was also carried out using the potentiostat (Fig. 3). The electrolyte flowed in a batch recirculating system, with the temperature maintained between 27 and $32 \text{ }^\circ\text{C}$ using a thermostatic bath. The cell voltage was continuously monitored to calculate the energy consumption. Most of the CC and MC + CC experiments were performed in triplicate. From these data, the standard deviations for

the different conditions were calculated.

The TOC contents of the samples collected during the electrolysis were analyzed using a Sievers InnovOx 900 analyzer (GE Analytical Instruments). Additionally, phenol and its aromatic intermediates benzoquinone, hydroquinone, and catechol were analyzed by HPLC (LC-20 Modular HPLC, Shimadzu), according to the methodology described by Andrade *et al.* (2006), with adaptations. Briefly, the analyses were performed using a Phenomenex[®] C-18 column (5 μm , 100 \AA) with dimensions 150 mm \times 4.6 mm. The UV detector was operated at $\lambda = 254$ nm. The mobile phase was a mixture of 0.01 mol L⁻¹ KH₂PO₄ (pH adjusted to 3 with H₃PO₄) and methanol, in a proportion of 80:20 (V/V), at a flow rate of 1.0 mL min⁻¹.

4.3 LIMITING CURRENT DETERMINATION

Before starting the electrooxidation using the MC technique, galvanostatic electrolysis experiments were carried out at different flow velocities (0.14, 0.25, 0.38, 0.59, 0.69, and 0.97 m s⁻¹), in the presence and absence of the turbulence promoters, in order to determine both the optimal flow velocity and the mass transfer coefficients (k_m). These tests were performed using the experimental setup shown in Fig. 3, but the constant current source was employed instead of a potentiostat. Aliquots of electrolyte were removed for subsequent determination of the TOC and phenol concentrations.

A constant current of 0.84 A (30 mA cm⁻²) was applied to ensure that the process was under mass transfer conditions and allow the determination of k_m by the exponential fitting of the phenol concentration decay. The k_m values were obtained using Eq. (16), where $C_{Ph}(t)$ is the phenol concentration (mg L⁻¹) at time t (s), $C_{Ph,0}$ is the initial phenol concentration (mg L⁻¹), A is the electrode geometric area (m²), and V is the electrolyte volume (m³).

$$C_{Ph}(t) = C_{Ph,0} \exp\left(-\frac{k_m A}{V} t\right) \quad (16)$$

Using the values of k_m , the limiting current as a function of the phenol concentration was obtained according to Eq. (15).

The expression used to modulate the applied current as a function of electrolysis time, Eq. (17), was obtained combining Eqs. (15) and (16), considering the number of electrons required for the total mineralization of phenol (28 electrons), according to the stoichiometric balance shown in Eq. (18).

$$I_{app}(t) = n F k_m A C_{Ph,0} \exp\left(-\frac{k_m A}{V} t\right) \quad (17)$$



In the MC assays, Eq. (17) was used to set the current values during the electrolysis, employing the Autolab Nova 2.1.3 software, which automatically adjusted the value of I_{app} every 30 s. The current step was chosen based on the work of Oliveira *et al.* (2020), who found that using a smaller number of currents steps did not improve electrolysis performance.

4.4 PERFORMANCE METRICS

The electrooxidation performance was evaluated in terms of the mineralization current efficiency (ε) and the specific energy consumption (η), calculated according to Eqs. (19) and (20), respectively. In these equations, $\Delta(TOC)_{exp}$ is the experimental variation of TOC ($mg\ L^{-1}$) when an amount of charge (Q_{app}) is applied (A s), E_{cell} is the average cell potential over a given time interval (V), M_c is the molar weight of carbon ($mg\ mol^{-1}$), and n_c is the number of carbon atoms in the molecule.

$$\varepsilon = \frac{n F V \Delta(TOC)_{exp}}{M_c n_c Q_{app}} \cdot 100 \quad (19)$$

$$\eta = \frac{1000 E_{cell} Q_{app}}{V \Delta(TOC)_{exp}} \quad (20)$$

The TOC depletion curves were also analyzed by fitting a pseudo-first-order kinetic model, represented by Eq. (21), where $k_{(TOC)}$ is the apparent kinetic constant.

$$TOC(t) = TOC_0 \exp(-k_{(TOC)} t) \quad (21)$$

5. RESULTS AND DISCUSSION

Previously, Oliveira *et al.* (2020) demonstrated a remarkable reduction of the specific energy consumption (79.5%) applying the MC mode, compared to the CC mode, for the electrooxidation of a synthetic solution of caffeic acid (a model phenolic compound) and a real coffee processing wastewater. However, the time required to achieve the same TOC removal increased by ~70%. Here, to overcome this drawback, an investigation was made using different turbulence promoters combined with the MC, CC, and MC + CC operational modes, which could improve the mass transfer coefficient and increase the limiting current, and accelerate the mineralization kinetics. Firstly, as a function of the flow velocity, the mass transfer coefficient was determined for the mesh turbulence promoter to identify the best flow rate condition for the operation of the electrochemical reactor.

5.1 DETERMINATION OF THE MASS TRANSFER COEFFICIENTS

As is known, k_m is a monotonically asymptotic function of the flow velocity (u), with no significant changes in its value being expected after a particular value of u . The selection of the optimum flow velocity to be applied for the MC electrolysis using the MTP as a turbulent promoter was based on the normalized phenol concentration decay over time for different flow velocities (Fig. 4(A)). The applied current chosen was sufficiently high to ensure that the process was under the mass transfer condition in order to be able to use Eq. (16) to determine k_m . Accordingly, the exponential decay ($R^2 > 0.98$) confirmed that the phenol degradation was under mass transfer control. The TOC depletion curves (Fig. 4(B)) were also well fitted following pseudo-first-order kinetics, according to Eq. 21. It should be noted that the process was very reproducible, with standard deviations of $\pm 1.6\%$ and $\pm 4.7\%$ for the phenol and TOC concentrations, respectively.

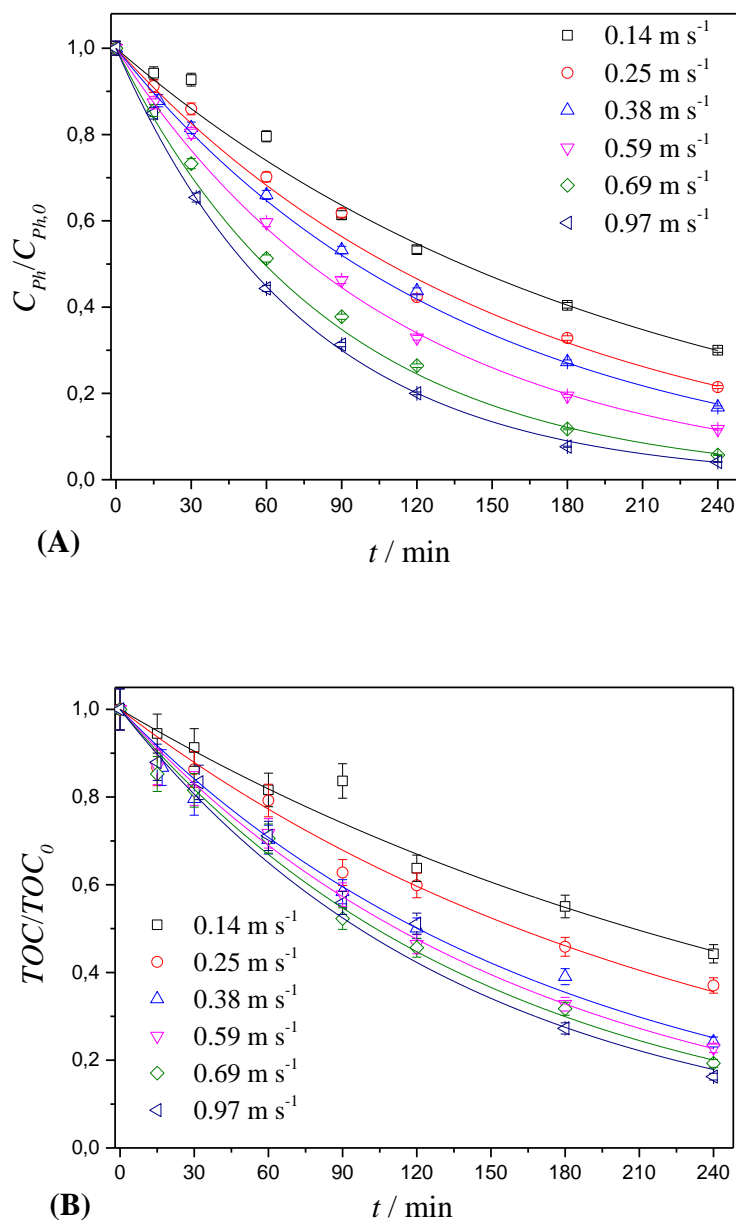


Fig. 4. Plots of the normalized phenol (A) and TOC (B) concentrations, as a function of time, for different flow velocities. Electrolysis conditions: $C_{Ph,0} = 130.6 \text{ mg L}^{-1}$ in 0.1 mol L^{-1} Na_2SO_4 ; $\text{TOC}_0 = 100 \text{ mg L}^{-1}$; $i = 30 \text{ mA cm}^{-2}$; $V = 1.4 \text{ L}$. Turbulence promoter: MTP.

Fig. 5 shows the plots of k_m and $k_{(\text{TOC})}$, as a function of flow velocity, and their respective values are shown in Table 3, as well as the values of the diffusive layer thickness (δ) calculated from the diffusion coefficient of phenol determined by Souza (2012).

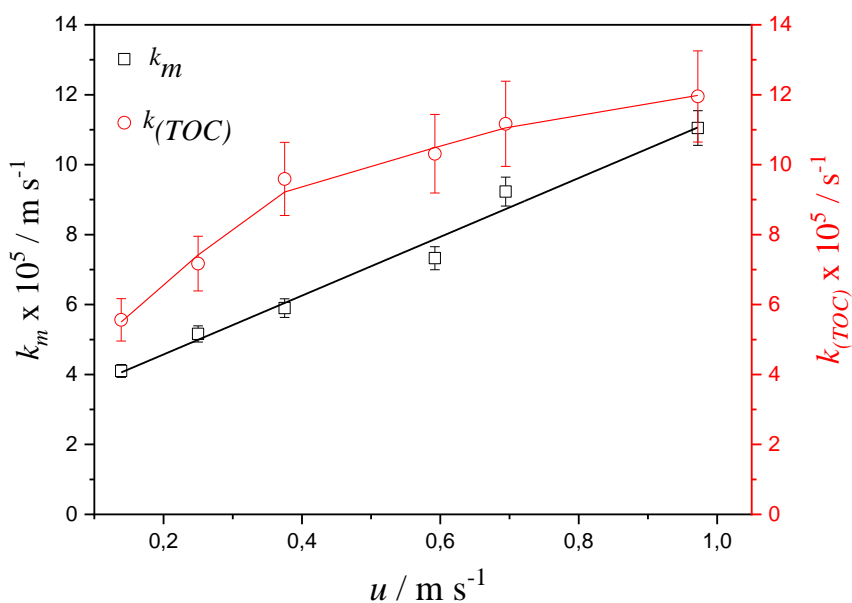


Fig. 5. Plots of k_m and $k_{(TOC)}$, as a function of flow velocity. Electrolysis conditions: $C_{Ph,0} = 130.6 \text{ mg L}^{-1}$ in $0.1 \text{ mol L}^{-1} \text{ Na}_2\text{SO}_4$; $TOC_0 = 100 \text{ mg L}^{-1}$; $i = 30 \text{ mA cm}^{-2}$; $V = 1.4 \text{ L}$. Turbulence promoter: MTP.

Table 3. Values of k_m , δ , and $k_{(TOC)}$ for the processes with turbulence promoter (MTP).

| $u / \text{m s}^{-1}$ | $k_m \times 10^5 / \text{m s}^{-1}$ | $\delta \times 10^5 / \text{m}^*$ | $k_{(TOC)} \times 10^5 / \text{s}^{-1}$ |
|-----------------------|-------------------------------------|-----------------------------------|---|
| 0.14 | 4.1 ± 0.2 | 3.1 ± 0.1 | 5.6 ± 0.6 |
| 0.25 | 5.2 ± 0.2 | 2.5 ± 0.1 | 7.2 ± 0.8 |
| 0.38 | 5.9 ± 0.3 | 2.2 ± 0.1 | 10 ± 1 |
| 0.59 | 7.3 ± 0.3 | 1.75 ± 0.08 | 10 ± 1 |
| 0.69 | 9.2 ± 0.4 | 1.39 ± 0.06 | 11 ± 1 |
| 0.97 | 11.1 ± 0.5 | 1.16 ± 0.05 | 12 ± 1 |

* $\delta (= D/k_m)$: diffusive layer thickness. D is the diffusion coefficient for phenol ($D = 1.28 \times 10^{-9} \text{ m}^2 \text{ s}^{-1}$, Souza (2012)).

The plot of k_m against u (Fig. 5) showed a linear increase of k_m as the flow velocity increased. On the other hand, considering the TOC depletion shown in Fig. 4(B) and Table 3, a different trend was observed in terms of $k_{(TOC)}$ (Fig. 5). Considering that the main purpose of the electrooxidation process was to remove TOC rather than to degrade phenol, a flow velocity of 0.69 m s^{-1} was selected in the subsequent electrolysis since the use of higher values of u would not lead to any significant improvement of $k_{(TOC)}$.

The mineralization process proceeds according to a complex mechanism involving the formation and electrooxidation of intermediates (Figs. 6 and 7). Depending on the flow rate and current density, the number of hydroxyl radicals on the electrode surface available to oxidize phenol or the intermediates will govern the degree of mineralization, as well as the mass transfer of phenol and intermediates to the electrode surface or back to the bulk medium (VEROLI, 2017).

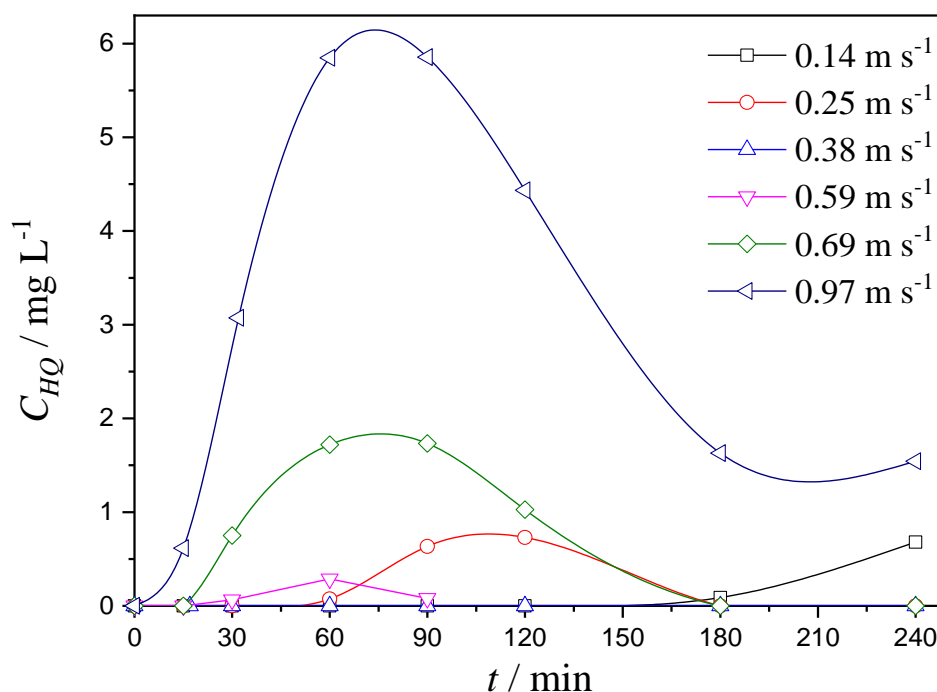


Fig. 6. Hydroquinone (C_{HQ}) concentrations against time for the electrolysis carried out at different flow velocities using the turbulence promoter MTP. Electrolysis conditions: $C_{Ph,0} = 130.6 \text{ mg L}^{-1}$ in $0.1 \text{ mol L}^{-1} \text{ Na}_2\text{SO}_4$; $i = 30 \text{ mA cm}^{-2}$; $V = 1.4 \text{ L}$.

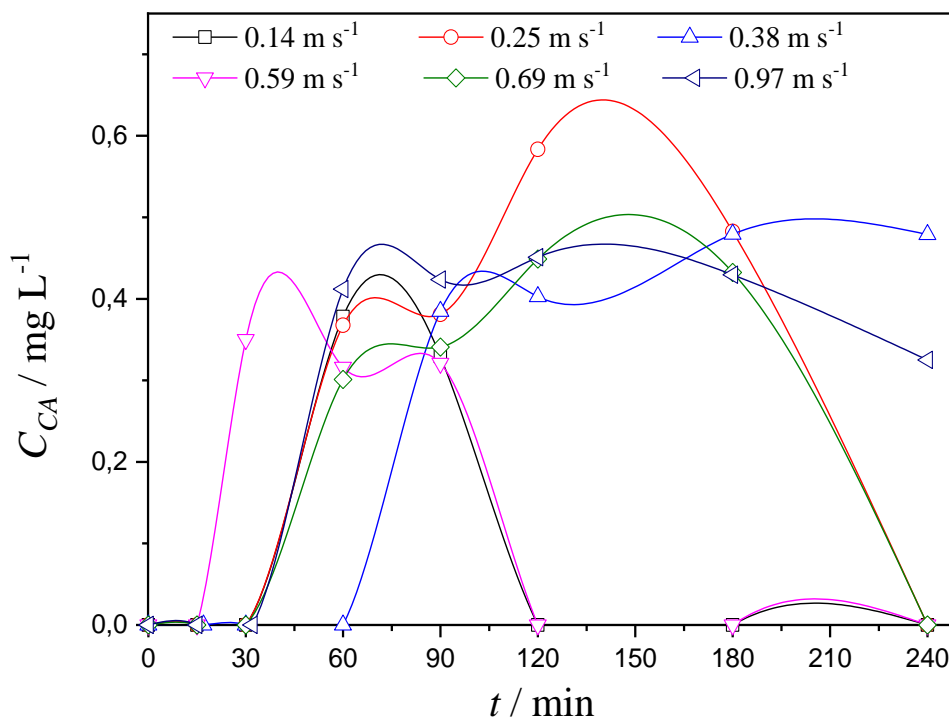


Fig. 7. Catechol (C_{CA}) concentrations against time for the electrolysis carried out at different flow velocities using the turbulence promoter MTP. Electrolysis conditions: $C_{Ph,0} = 130.6 \text{ mg L}^{-1}$ in $0.1 \text{ mol L}^{-1} \text{ Na}_2\text{SO}_4$; $i = 30 \text{ mA cm}^{-2}$; $V = 1.4 \text{ L}$.

As shown in Fig. 6, the total quinones component (see discussion below), here represented only by hydroquinone (HQ), was identified as the primary aromatic intermediate formed during the electrolysis, with its concentration (up to 6 mg L^{-1}) depending on the flow velocity. Catechol was also detected (Fig. 7), but at much lower concentrations ($< 0.6 \text{ mg L}^{-1}$). These results were in good agreement with those reported by Weiss *et al.* (2008). They identified hydroquinone, catechol, and benzoquinone as the main intermediates during phenol degradation, with the concentration of each compound depending on the catalytic activity of the anode and the reactor configuration.

Although substantial amounts of HQ were observed, benzoquinone was not identified in the samples. This outcome could be explained by the benzo/hydroquinone redox couple reacting reversibly between the electrodes, as well as the possible formation of a phenol

oligomer with the same retention time as HQ (WEISS *et al.*, 2008). For these reasons, the HQ concentrations shown in Fig. 6 are representative of the trend. A higher amount of HQ was detected at high flow velocities, indicating that, although the same amount of hydroxyl radicals was formed (since the same current density was applied), there was a tradeoff between the quantity of HQ available on the electrode surface for reaction to form more oxidized compounds (carboxylic acids or even mineralization) and the amount that diffused back to the bulk solution. For instance, at 0.97 m s^{-1} , phenol was oxidized to HQ, but it diffused back to the bulk solution more easily, because the diffusive layer was compressed and thinner at high flow velocities (Table 3). Consequently, the mass transfer of HQ from the surface to the bulk solution was enhanced, resulting in the detection of higher HQ concentrations. On the other hand, at 0.14 m s^{-1} , HQ was almost undetectable, suggesting that phenol was rapidly degraded to more oxidized compounds on the electrode surface.

The same approach was employed to determine k_m for the processes with RVC and without a turbulence promoter. In the absence of a TP, at 0.69 m s^{-1} , the value of k_m was $4.8 \pm 0.2 \times 10^{-5} \text{ m s}^{-1}$, in close agreement with the value of $4.6 \times 10^{-5} \text{ m s}^{-1}$ obtained by Souza (2012) and applied by Oliveira *et al.* (2020), using the same electrochemical reactor, but employing the ferricyanide/ferrocyanide redox couple technique.

A further investigation was performed using the 45 ppi RVC as a turbulence promoter, but applying 0.59 m s^{-1} to save energy in the pumping operation. This assessment was made considering that even applying a flow velocity lower than 0.69 m s^{-1} , the k_m value obtained using the RVC would be higher than that observed for the MTP, due to the influence of the porous matrix on the turbulence flow pattern, as discussed further below. This behavior highlights the effectiveness of a consolidated porous medium, such as RVC, in improving electrooxidation kinetics under galvanostatic conditions (FARINOS and RUOTOLO, 2017; RECIO *et al.*, 2011; RAMÍREZ *et al.*, 2016).

5.2 COMPARISON OF THE DIFFERENT TURBULENCE PROMOTERS

The process performance was first evaluated using the different turbulence promoters, at 0.69 m s^{-1} , under galvanostatic conditions. As expected (Figs. 8 and 9), the turbulence

promoters increased the degradation kinetics of both phenol and TOC due to the enhanced mass transfer. The k_m values (Table 4) revealed that the RVC was more effective than the MTP, which could be attributed to the effect of the 3D matrix in creating higher inertial forces that promoted greater turbulence. However, the porosity and thickness of the RVC did not significantly affect the mass transfer, as evidenced by the γ values for the experiments performed at 0.59 m s^{-1} (Table 4). In terms of $k_{(TOC)}$, the MTP provided a 1.6-fold increase of the TOC depletion kinetics, while the use of the RVC led to an average improvement of ~2.5-fold for the same flow velocity. For both MTP and RVC, the values of γ (Table 4) were close to those found by Wachter (2019) (between 1.5 and 2.9), who compared the use of one, two, and three (overlapping in the last two cases) polymeric turbulence promoters for the degradation of bisphenol S at 0.61 m s^{-1} . Interestingly, the use of overlapping promoters provided an increase of k_m similar to that obtained using the RVC in the present work.

The type, shape, and mesh layout of the turbulence promoter influence the degree of mass transfer improvement (WACHTER, 2019; BROWN *et al.*, 1993). In general, tight meshes provide greater turbulence due to higher inertial forces caused by the contact between the electrolyte and the TP, changing the flow trajectory (BROWN *et al.*, 1993). This fact probably explained the higher efficiency of the RVC as a TP compared to the MTP. The small pore size of the 60 ppi RVC could also explain the increase in the degradation rate, compared to the 45 ppi RVC (Fig. 9(B)). Considering the RVC thickness, the small improvements of k_m and $k_{(TOC)}$ provided by increasing the thickness from 2.5 to 5.0 mm would not be sufficient to justify the use of the greater thickness due to the higher cost of the TP. Considering all these results, the 45 ppi RVC with 2.5 mm thickness was chosen for further investigation as a turbulence promoter, using the modulated current mode.

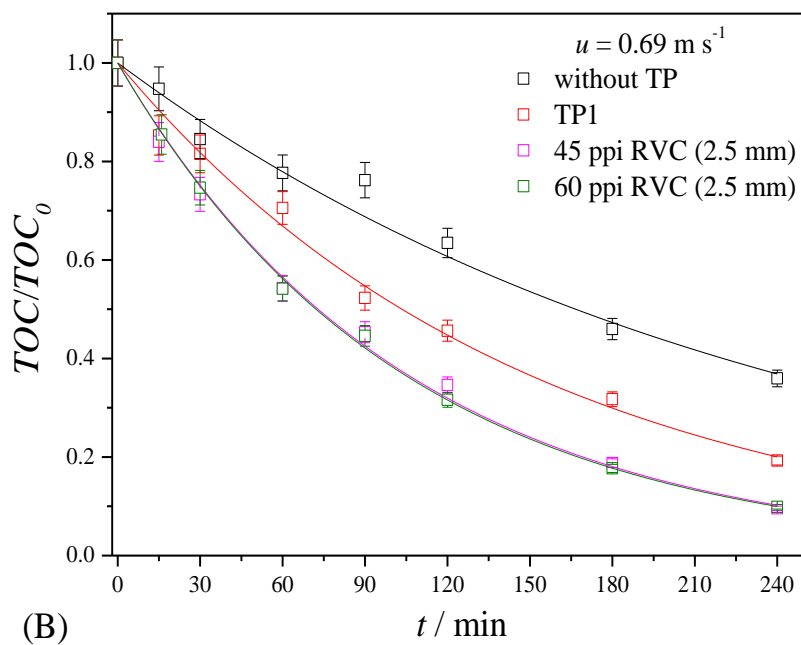
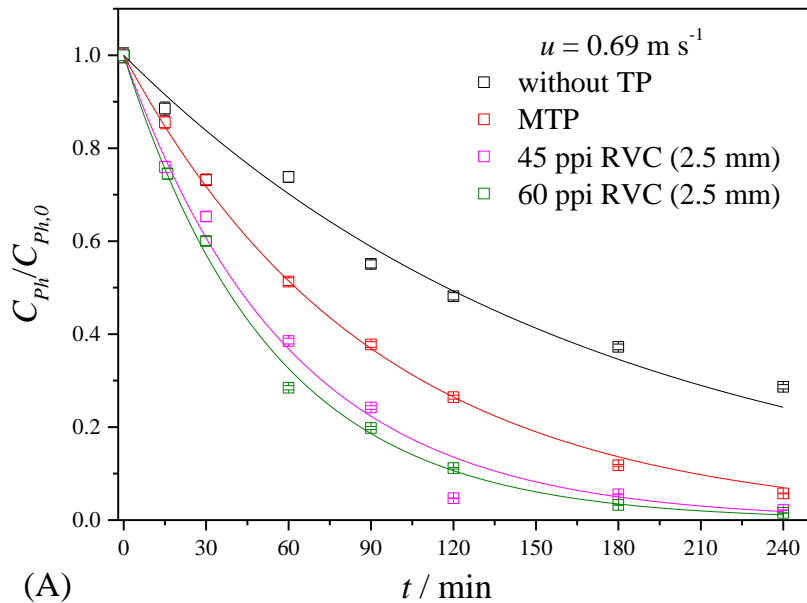


Fig. 8. (A) Normalized phenol and (B) TOC depletion, according to time, for the electrochemical reactor operating in the absence and presence of different turbulence promoters, using flow velocity (u) of 0.69 m s^{-1} , with $i = 30 \text{ mA cm}^{-2}$. The lines represent the fitted models, according to Eqs. (16) and (21).

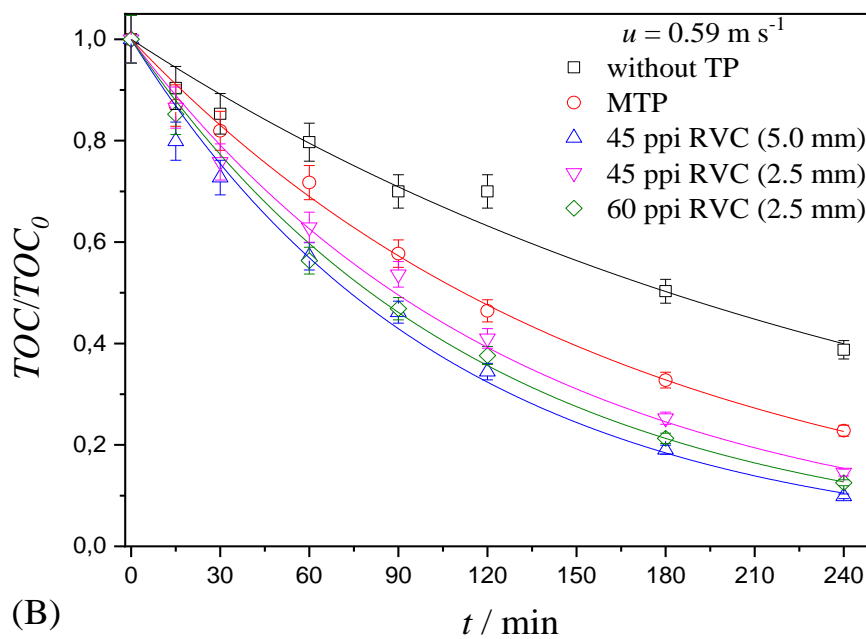
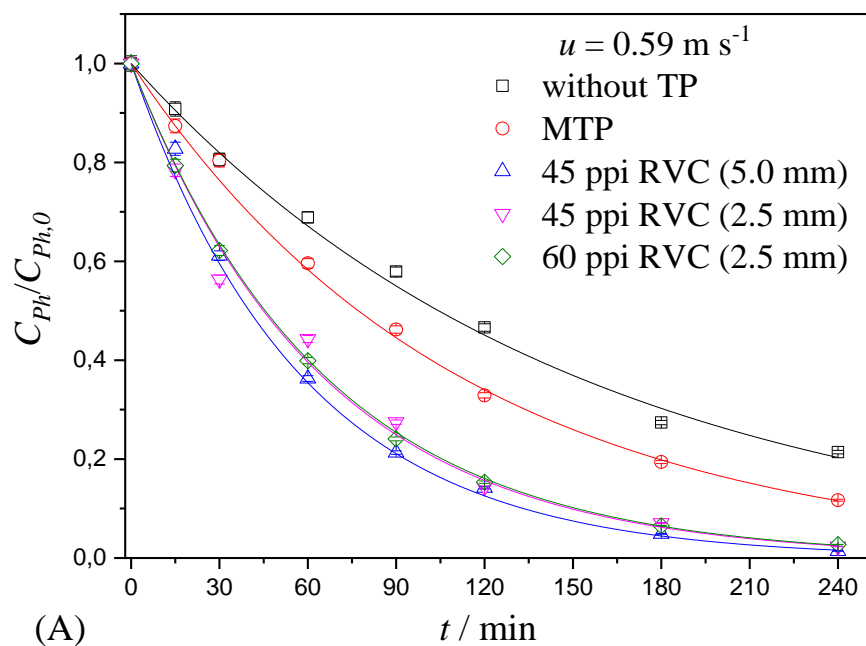


Fig. 9. (A) Normalized phenol and (B) TOC depletion, according to time, for the electrochemical reactor operating in the absence and presence of different turbulence promoters, using flow velocity (u) of 0.59 m s^{-1} , with $i = 30 \text{ mA cm}^{-2}$. The lines represent the fitted models, according to Eqs. (16) and (21).

Table 4. Values of k_m , γ , and $k_{(TOC)}$ for the processes carried out using different turbulence promoters and flow velocities.

| Turbulence promoter | u (m s ⁻¹) | $k_m \times 10^5$ (m s ⁻¹) | γ | $k_{(TOC)} \times 10^5$ (s ⁻¹) |
|---------------------|--------------------------|--|------------|--|
| Without TP | | 5.4 ±0.2 | - | 6.3 ±0.7 |
| MTP | | 7.3 ±0.3 | 1.35 ±0.09 | 10 ±1 |
| 45 ppi RVC (5.0 mm) | 0.59 | 13.7 ±0.6 | 2.5 ±0.2 | 16 ±2 |
| 45 ppi RVC (2.5 mm) | | 12.8 ±0.6 | 2.4 ±0.1 | 13 ±1 |
| 60 ppi RVC (2.5 mm) | | 13.0 ±0.6 | 2.4 ±0.2 | 14 ±2 |
| Without TP | | 4.8 ±0.2 | - | 6.7 ±0.7 |
| MTP | 0.69 | 9.2 ±0.4 | 1.9 ±0.1 | 11 ±1 |
| 45 ppi RVC (2.5 mm) | | 13.9 ±0.6 | 2.9 ±0.2 | 16 ±2 |
| 60 ppi RVC (2.5 mm) | | 15.6 ±0.7 | 3.2 ±0.2 | 16 ±2 |

5.3 ELECTROOXIDATION COMBINING MODULATED CURRENT AND TURBULENCE PROMOTERS

The equations used to modulate the applied current were established based on Eq. (17), using the values of k_m displayed in Table 4 for the processes carried out without any TP (Eq. 22) or with the MTP (Eq. 23) and the 45 ppi RVC (Eq. 24). In the application of these equations, it was hypothesized that the degradation kinetics of phenol and its intermediates, under mass transfer control, was independent of the nature of the organic molecule, so the value of k_m could be considered constant throughout the electrolysis. Additionally, the contribution of oxidation in the bulk solution to the degradation was considered negligible. Kapalka *et al.* (2008) demonstrated that this simplification would have a minor impact on the limiting current since the reaction rate with the hydroxyl radicals is very fast and controlled by mass transfer.

$$I_{app}(t) = 0.48 \exp(-9.19 \times 10^{-5} t) \quad (22)$$

$$I_{app}(t) = 0.97 \exp(-1.85 \times 10^{-4} t) \quad (23)$$

$$I_{app}(t) = 1.34 \exp(-2.56 \times 10^{-4} t) \quad (24)$$

Fig. 10 shows the electrolysis results using modulated current, under different conditions, expressed in terms of the normalized TOC depletion according to time. The process using MC mode was also highly reproducible, with a standard deviation of $\pm 3.6\%$. When using the current modulation technique, the applied current density reached very low values after a certain period of electrolysis, leading to electrode potentials that prevented the formation of hydroxyl radicals, so the degradation of organics ceased. Panizza and coworkers (2008) reported that BDD anodes must operate at potentials higher than 2.0 V vs. SHE, which usually means operating with applied current densities above 5 mA cm⁻², to avoid interruption of the degradation and deactivation of the electrode. Considering this limitation, preliminary experiments in MC mode were carried out to define the modulation time and the minimum current densities that could be applied. The subsequent experiments combined the modulated and galvanostatic approaches (MC + CC electrolysis).

Here, for the process operating in MC mode, in the absence and presence of the MTP, the degradations were no longer observed during the periods 360-420 min and 240-300 min of electrolysis, respectively. Hence, in the electrolysis applying the MC + CC modes, the current was modulated over 300 min and 180 min, in the absence and presence of MTP, which corresponded to current densities of ~ 3.6 mA cm⁻² (100 mA) and ~ 4.6 mA cm⁻² (130 mA), respectively. Once these currents had been reached, the process was operated galvanostatically, as indicated by the full lines in Fig. 10. Oliveira *et al.* (2020) observed a similar trend for an electrochemical reactor used for caffeic acid degradation, without a turbulence promoter and at a higher flow velocity (1.1 m s⁻¹).

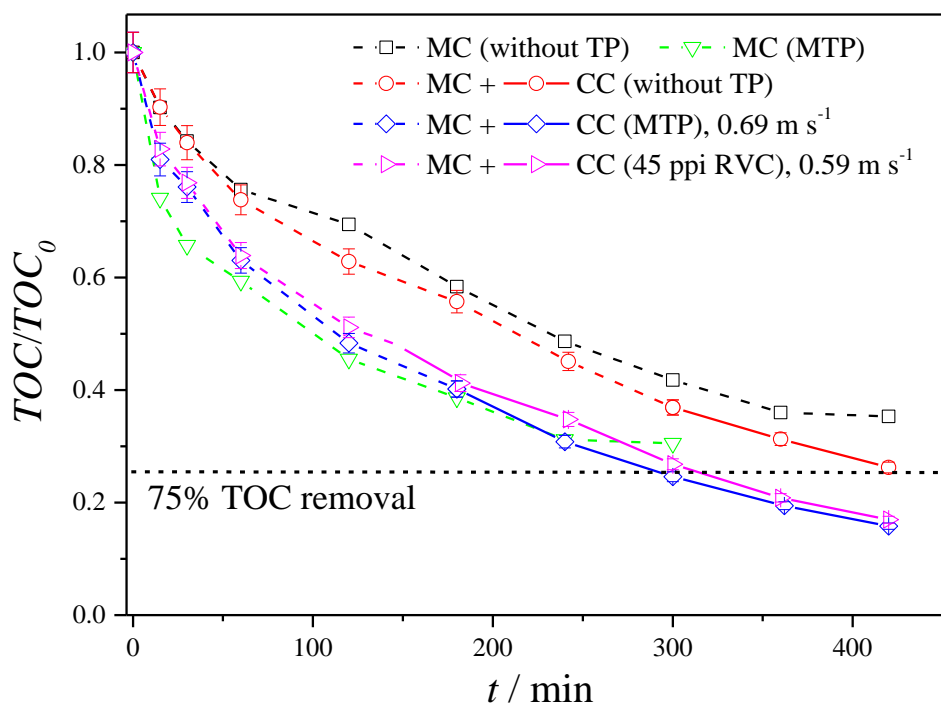


Fig. 10. Normalized TOC values, according to time, for the processes carried out using the MC and MC + CC modes, in the absence and presence of different turbulence promoters. Electrolysis conditions: $C_{Ph,0} = 130.6 \text{ mg L}^{-1}$ in $0.1 \text{ mol L}^{-1} \text{ Na}_2\text{SO}_4$; $TOC_0 = 100 \text{ mg L}^{-1}$; $V = 1.4 \text{ L}$; $I_{0app} = 0.48 \text{ A}$ (without TP), $I_{0app} = 0.97 \text{ A}$ (MTP), and $I_{0app} = 1.34 \text{ A}$ (45 ppi RVC).

The comparison of the processes showed that operating in MC + CC mode significantly reduced the time required to achieve the same TOC removal when turbulence promoters were used. For example, the time required for 75% TOC removal was reduced from approximately 420 min to 295 min (around 30% shorter), irrespective of the turbulence promoter employed. Compared to the behavior observed using CC mode (Figs. 8 and 9), the difference between the effects of the MTP and the 45 ppi RVC was less evident for MC + CC mode. Hence, the MTP would be the best option in terms of simplicity and cost, even applying a high flow velocity.

In summary, the main drawbacks concerning the use of the MC + CC mode, as reported previously (OLIVEIRA *et al.*, 2020), which are the longer operational time or the requirement for larger anodes, can be easily compensated using low-cost mesh turbulence

promoters. The electrolysis time was lower using the CC mode combined with MTP (Figs. 8 and 9), but in this case, the advantage of low specific energy consumption was lost (Table 5), since part of the applied current was diverted towards parasitic reactions, such as the oxygen evolution reaction (OER).

Fig. 11(A) shows the applied current, according to electrolysis time, for the processes carried out using the CC and MC + CC modes, without and with the TP. The applied charges shown in the graph were calculated by integrating the areas below the curves, considering 75% TOC depletion (Fig. 10), and were used to calculate the values of ε and η (Table 5), together with the average values of E_{cell} (Fig. 11(B)). Calculation of the mineralization current efficiency and the specific energy consumption considered the time necessary to remove a stipulated percentage of the initial TOC content. As a consequence of the mass transfer enhancement provided by the turbulence promoter, the mineralization was more efficient, resulting in substantially lower energy consumption compared to the galvanostatic electrooxidation.

Interestingly, for the process performed using the MC + CC mode, the mineralization efficiencies were very similar in the absence or presence of the MTP. However, there was no decrease in energy consumption using the turbulence promoter, as would be expected, with the values for the two conditions (with and without TP) being statistically the same. This could be attributed to an additional ohmic drop introduced by the plastic mesh, as confirmed by the slightly higher E_{cell} value (Table 5) observed for this electrolysis condition. Therefore, the main advantage of using the turbulence promoter was the shorter time required for mineralization.

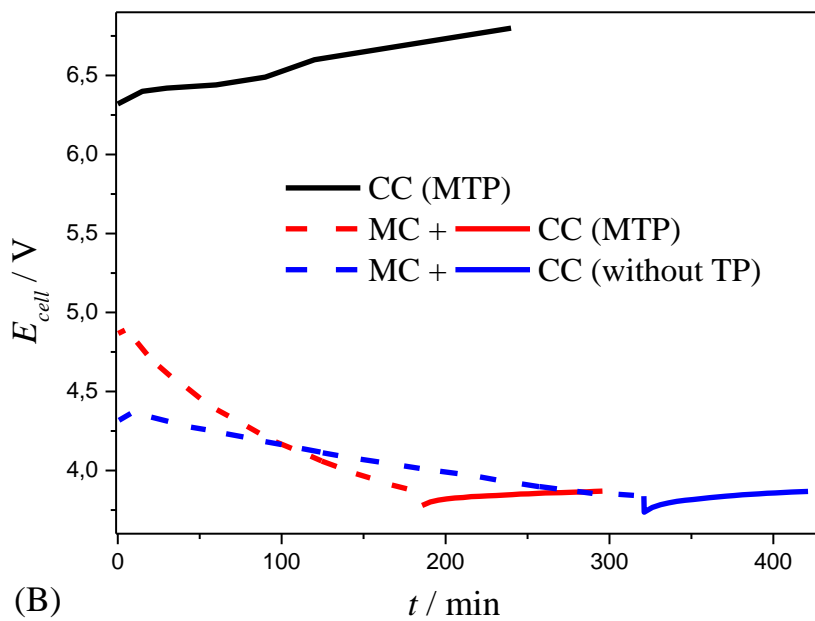
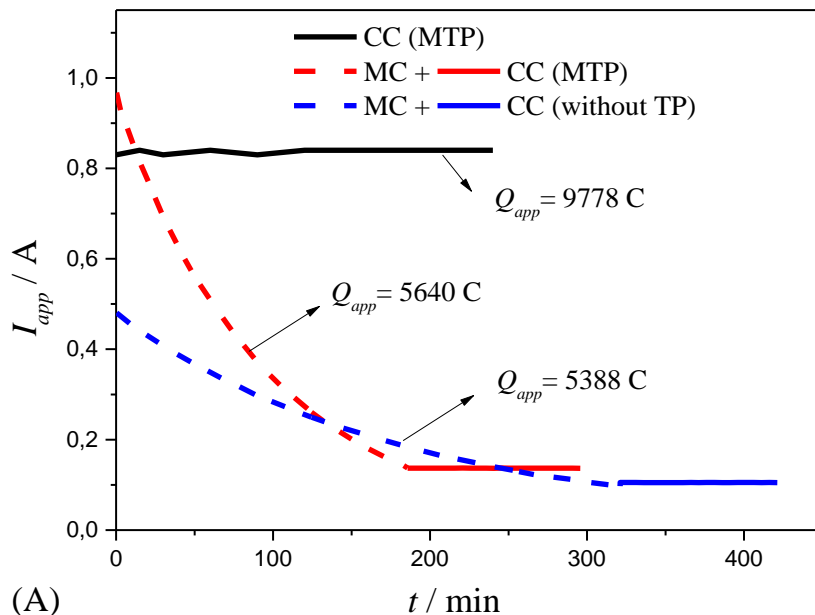


Fig. 11. Plots of (A) the applied current and (B) the cell potential, according to time, for the processes using CC and MC + CC modes. The charge values correspond to 75% TOC removal.

Table 5. Values of ε , η , E_{cell} , and t for the processes using CC and MC + CC modes, in the presence and absence of the MTP, considering 75% TOC removal.

| Electrolysis condition | ε (%) | η (kWh kg ⁻¹ TOC) | E_{cell} (V) | t (min) |
|------------------------|-------------------|-----------------------------------|----------------|-----------|
| CC (MTP) | 41 ±7 | 168 ±31 | 6.52 | 203 |
| MC + CC (MTP) | 62 ±6 | 72 ±6 | 4.18 | 295 |
| MC + CC (without TP) | 63 ±5 | 66 ±5 | 4.06 | 420 |

The trends shown in Table 5 were in agreement with the work of Oliveira *et al.* (2020), employing a similar electrochemical reactor for the mineralization of caffeic acid (120 mg L⁻¹ TOC), but without a turbulence promoter, where the use of the MC + CC mode resulted in ε and η of 77% and 52 kWh kg⁻¹, respectively, for 64% TOC removal. This further evidenced that these metrics were slightly influenced by the presence of the turbulence promoter, considering similar values of TOC_0 and TOC removal. On the other hand, Oliveira *et al.* (2020) found that the use of the MC + CC mode increased the mineralization time by ~69% (from 7.1 to 12 h) for the same volume of electrolyte. In the present work, with the MTP, the time required for mineralization using the MC + CC mode was ~45% longer than for the process operated under CC.

Finally, the energy cost was estimated, considering the energy consumption for 75% TOC removal and assuming a value of 0.14 US\$/kWh (OLIVEIRA *et al.*, 2020). For the galvanostatic process with MTP, the energy required to treat 1.0 m³ of electrolyte was between 11.5 and 14.4 kWh, leading to a treatment cost of 1.61-2.02 US\$/m³. However, this cost was considerably reduced using the MC + CC mode, with values of 0.64-0.68 US\$/m³ (4.54-4.83 kWh m⁻³) for the MTP system and 0.59-0.63 US\$/m³ (4.21-4.48 kWh m⁻³) for the system without TP, which confirmed the expected economic gain achieved by applying the current modulation method.

Table 6 shows some results found in the literature for galvanostatic electrodegradation of phenol, for different electrodes and specific operating conditions, as well as the results obtained by the present work using MTP and under MC + CC mode.

Table 6. Comparison of galvanostatic electrooxidation of phenol under different conditions.

| Electrode | Conditions | i (mA cm ⁻²) | t (min) | Efficiency | Energy consumption | Reference |
|----------------------|--|--|--------------|--|--|-------------------------------------|
| Ti/RuO ₂ | 200 mg L ⁻¹ phenol, 0.1 mol L ⁻¹ Na ₂ SO ₄ , 500 mL | 15 | 50 | 100% removal efficiency (85.4% COD removal) | 150.3 kWh m ⁻³ | Yavuz and Koparal (2006) |
| PbO ₂ | 1882.2 mg L ⁻¹ phenol, 0.1 mol L ⁻¹ H ₂ SO ₄ | 142 | 300 | 99% removal of phenol and its aromatic intermediaries | 330 kWh m ⁻³ | Weiss <i>et al.</i> (2008) |
| BDD | | 47 | | | 80 kWh m ⁻³ | |
| BDD | 540 mg L ⁻¹ COD (~226.9 mg L ⁻¹ phenol), 0.1 mol L ⁻¹ Na ₂ SO ₄ | 20 | 180 | 75.9% COD removal (from 540 mg L ⁻¹ to 130 mg L ⁻¹) | 34.76 kWh m ⁻³ | Zhu <i>et al.</i> (2011) |
| PbO ₂ | 50 mg L ⁻¹ phenol, 0.05 mol L ⁻¹ Na ₂ SO ₄ , 200 mL | 50 | 180 | 100% removal efficiency | 3759 kWh kg ⁻¹ TOC | Duan <i>et al.</i> (2013) |
| RVC/PbO ₂ | 214 mg L ⁻¹ TOC (~279.7 mg L ⁻¹) phenol, 0.1 mol L ⁻¹ Na ₂ SO ₄ | 30 | 480 | 95% COT removal | ~5.7 kWh m ⁻³ | Farinos and Ruotolo (2017) |
| BDD | 130.6 mg L ⁻¹ phenol, 0.1 mol L ⁻¹ Na ₂ SO ₄ , 1400 mL | MC + CC (from 34.6 to 4.6) | 295 | 75% COT removal | 72 ±6 kWh kg ⁻¹ TOC (4.54- 4.83 kWh m ⁻³) | This work |

Although the comparison between these results cannot be made directly, since they are dependent on different parameters (e.g., electrode potential and material, current densities, and mass transport) some considerations can be made. It is possible to observe in Table 6 the greater efficiency, as expected, of the BDD than the oxide electrodes, considering similar electrolytes, as well as the efficiency of the three-dimensional RVC/PbO₂ electrodes in the study of Farinos and Ruotolo (2017). Additionally, the low energy consumption of the

process studied in this research (MC + TP) is remarkable compared to the results of Yavuz and Koparal (2006), Zhu *et al.* (2011), and Duan *et al.* (2013), for example, which have similarities concerning the initial concentration of phenol and supporting electrolyte. This reinforces the potential of the method studied, demonstrating that the combination of TP and MC is a simple and effective alternative in reducing the energy cost in electrooxidation processes of effluents containing organic pollutants.

6. CONCLUSIONS

Given the results obtained and discussed in this research, the following conclusions were formulated for studies to optimize the phenol electrooxidation process in an electrochemical flow reactor, combining the use of turbulence promoters and current modulation.

From the galvanostatic electrolysis using the different turbulence promoters evaluated, it was possible to observe the greater efficiency of RVC than MTP to promote turbulence and increase the degradation kinetics. However, this difference was less pronounced when the process was carried out using modulated current, with a lesser influence on the type of promoter being observed for this operational regime. Thus, similar performance could be achieved using the MTP compared to the process using the RVC by slightly increasing the flow velocity.

The proposed approach combining turbulence promoters and the modulated current was successful in reducing the electrolysis time required by ~30% while maintaining low energy consumption. Considering 75% of TOC removal, the energy consumption decreased from 168 ± 31 kWh kg⁻¹ TOC for the CC process to 72 ± 6 kWh kg⁻¹ TOC for the MC + CC mode, using a simple and inexpensive plastic mesh turbulence promoter. These results highlight the importance of using turbulence promoters to optimize the degradation kinetics of organic compounds, showing how the TP layout can influence the electrochemical process.

7. SUGGESTIONS FOR FUTURE RESEARCH

- Study the scale-up of the electrooxidation process of organic compounds;
- Develop an in-depth cost-benefit analysis, also considering the process on an industrial scale;
- Investigate the use of lower-cost electrodes compared to BDD in processes using modulated current and turbulence promoters;
- Study the application of the evaluated method (combining MC and TP) in the electrochemical treatment of real effluents;
- Evaluate the economic viability of the coupling of electrochemical treatments and adsorption.

REFERENCES

ANDRADE, L. S.; LAURINDO, E. A.; DE OLIVEIRA, R. V.; ROCHA-FILHO, R. C.; CASS, Q. B. Development of a HPLC method to follow the degradation of phenol by electrochemical or photoelectrochemical treatment. **Journal of the Brazilian Chemical Society**, v. 17, n. 2, p. 369-373, 2006.

ANGLADA, A.; URTIAGA, A.; ORTIZ, I. Contributions of electrochemical oxidation to waste-water treatment: fundamentals and review of applications. **Journal of Chemical Technology & Biotechnology**, v. 84, n. 12, p. 1747-1755, 2009.

ATHARIZADE, M.; MIRANZADEH, M. B. Evaluation of efficacy of advanced oxidation processes Fenton, Fenton-like and photo-Fenton for removal of phenol from aqueous solutions. **Journal of the Chemical Society of Pakistan**, v. 37, n. 02, p. 266, 2015.

AYOUB, H.; ROQUES-CARMES, T.; POTIER, O.; KOUBAISSY, B.; PONTVIANNE, S.; LENOUVEL, A.; GUIGNARD, C.; MOUSSET, E.; POIROT, H.; TOUFAILY, J.; HAMIEH, T. Iron-impregnated zeolite catalyst for efficient removal of micropollutants at very low concentration from Meurthe river. **Environmental Science and Pollution Research**, v. 25, n. 35, p. 34950-34967, 2018.

BANERJEE, A.; GHOSHAL, A. K. Phenol degradation by *Bacillus cereus*: pathway and kinetic modeling. **Bioresource Technology**, v. 101, n. 14, p. 5501-5507, 2010.

BAZRAFSHAN, E.; BIGLARI, H.; MAHVI, A. H. Phenol removal by electrocoagulation process from aqueous solutions. **Fresenius Environmental Bulletin**, v. 21, n. 2, p. 364-371, 2012.

BELLO, M. M.; RAMAN, A. A. A.; ASGHAR, A. A review on approaches for addressing the limitations of Fenton oxidation for recalcitrant wastewater treatment. **Process Safety and Environmental Protection**, 2019.

BIGLARI, H.; AFSHARNIA, M.; ALIPOUR, V.; KHOSRAVI, R.; SHARAFI, K.; MAHVI, A. H. A review and investigation of the effect of nanophotocatalytic ozonation process for phenolic compound removal from real effluent of pulp and paper industry. **Environmental Science and Pollution Research**, v. 24, n. 4, p. 4105-4116, 2017.

BORA, L. V.; MEWADA, R. K. Visible/solar light active photocatalysts for organic effluent treatment: Fundamentals, mechanisms and parametric review. **Renewable and Sustainable Energy Reviews**, v. 76, p. 1393-1421, 2017.

BRASIL. Ministério do Meio Ambiente. Conselho Nacional do Meio Ambiente – CONAMA. Resolução nº 430, de 13 de maio de 2011. Dispõe sobre as condições e padrões de lançamento de efluentes, complementa e altera a Resolução nº 357, de 17 de março de 2005, do Conselho Nacional do Meio Ambiente - CONAMA. **Diário Oficial [da] República Federativa do Brasil**, Poder Executivo, Brasília, DF., n. 92, p. 89, 16 mar. 2011. Disponível em: <http://www2.mma.gov.br/port/conama/legiabre.cfm?codlegi=646>. Acesso em 23 set. 2019.

BRITTO, J. M.; RANGEL, M. C. Processos avançados de oxidação de compostos fenólicos em efluentes industriais. **Química Nova**, v. 31, n. 1, p. 114-122, 2008.

BRITTO-COSTA, P. H.; RUOTOLO, L. A. M. Electrochemical removal of copper ions from aqueous solutions using a modulated current method. **Separation Science and Technology**, v. 46, n. 7, p. 1205–1211, 2011.

BROWN, C. J.; PLETCHER, D.; WALSH, F. C.; HAMMOND, J. K.; ROBINSO, D. Studies of space-averaged mass transport in the FM01-LC laboratory electrolyser. **Journal of applied electrochemistry**, v. 23, n. 1, p. 38-43, 1993.

CARBAJO, J.; QUINTANILLA, A.; CASAS, J. A. Assessment of carbon monoxide formation in Fenton oxidation process: The critical role of pollutant nature and operating conditions. **Applied Catalysis B: Environmental**, v. 232, p. 55-59, 2018.

CAVALCANTE, P. R. M. **Remoção de fenol de efluentes aquosos utilizando floculação iônica**. 2016. Dissertação de Mestrado. Universidade Federal do Rio Grande do Norte.

CHAICHANAWONG, J.; YAMAMOTO, T.; OHMORI, T. Enhancement effect of carbon adsorbent on ozonation of aqueous phenol. **Journal of Hazardous Materials**, v. 175, n. 1-3, p. 673-679, 2010.

CHASIB, K. F. Extraction of Phenolic Pollutants (Phenol and p-Chlorophenol) from Industrial Wastewater. **Journal of Chemical & Engineering Data**, v. 58, n. 6, p. 1549-1564, 2013.

COMNINELLIS, C. Electrocatalysis in the electrochemical conversion/combustion of organic pollutants for waste water treatment. **Electrochimica Acta**, v. 39, n. 11-12, p. 1857-1862, 1994.

COMNINELLIS, C.; CHEN, G. **Electrochemistry for the Environment**. New York: Springer, 2010.

COMNINELLIS, C.; KAPALKA, A.; MALATO, S.; PARSONS, S. A.; POULIOS, I.; MANTZAVINOS, D. Advanced oxidation processes for water treatment: advances and trends for R&D. **Journal of Chemical Technology & Biotechnology**, v. 83, n. 6, p. 769-776, 2008.

DA SILVA, W. L.; LANSARIN, M. A.; LIVOTTO, P. R.; DOS SANTOS, J. H. Z. Photocatalytic degradation of drugs by supported titania-based catalysts produced from petrochemical plant residue. **Powder Technology**, v. 279, p. 166-172, 2015.

DE MELLO, R.; SANTOS, L. H. E.; PUPO, M. M. S.; EGUILUZ, K. I. B.; SALAZAR-BANDA, G. R.; MOTHEO, A. J. Alachlor removal performance of Ti/Ru 0.3 Ti 0.7 O 2 anodes prepared from ionic liquid solution. **Journal of Solid State Electrochemistry**, v. 22, n. 5, p. 1571-1580, 2018.

DOMINGUEZ-RAMOS, A.; IRABIEN, A. Analysis and modeling of the continuous electro-oxidation process for organic matter removal in urban wastewater treatment. **Industrial & Engineering Chemistry Research**, v. 52, n. 22, p. 7534-7540, 2013.

DUAN, X.; MA, F.; YUAN, Z.; CHANG, L.; JIN, X. Electrochemical degradation of phenol in aqueous solution using PbO₂ anode. **Journal of the Taiwan Institute of Chemical Engineers**, v. 44, n. 1, p. 95-102, 2013.

EYDIVAND, S.; NIKAZAR, M. Degradation of 1, 2-Dichloroethane in simulated wastewater solution: A comprehensive study by photocatalysis using TiO₂ and ZnO nanoparticles. **Chemical Engineering Communications**, v. 202, n. 1, p. 102-111, 2015.

FARINOS, R. M. **Preparação, caracterização e aplicação de eletrodos tridimensionais de carbono vítreo reticulado recobertos com filmes de PbO₂ para a degradação do corante reativo AR 19 e glifosato**. 2016. 175 f. Tese (Doutorado em Engenharia Química)

- Programa de Pós-Graduação em Engenharia Química, Universidade Federal de São Carlos, São Carlos, 2016.

FARINOS, R. M.; RUOTOLO, L. A. M. Comparison of the electrooxidation performance of three-dimensional RVC/PbO₂ and boron-doped diamond electrodes. **Electrochimica Acta**, v. 224, p. 32–39, 2017.

FARINOS, R. M.; ZORNITTA, R. L.; RUOTOLO, L. A. M. Development of three-dimensional electrodes of PbO₂ electrodeposited on reticulated vitreous carbon for organic electrooxidation. **Journal of the Brazilian Chemical Society**, v. 28, n. 1, p. 187–196, 2017.

FENG, Y; YANG, L.; LIU, J.; LOGAN, B. E. Electrochemical technologies for wastewater treatment and resource reclamation. **Environmental Science: Water Research & Technology**, v. 2, p. 800-831, 2016.

GHASEMIAN, S. **Development of Photoelectrochemicallyactive Tin-Tungsten Oxide Electrodes for Organic Wastewater Treatment and Water Disinfection**. 2017. 171 p. Tese (Doutorado em Engenharia Química) - Universidade McGill, Montreal, Quebec, Canada, 2017. Disponível em: http://digitool.library.mcgill.ca/webclient/StreamGate?folder_id=0&dvs=1570340739967~395. Acesso em: 27 set. 2019.

GHASEMY-PIRANLOO, F.; BAVARSIHA, F.; DADASHIAN, S.; RAJABI, M. Synthesis of core/shell/shell Fe₃O₄/SiO₂/ZnO nanostructure composite material with cubic magnetic cores and study of the photo-degradation ability of methylene blue. **Journal of the Australian Ceramic Society**, p. 1-9, 2019.

HADJLTAIEF, H. B.; ZINA, M. B.; GALVEZ, M. E.; DA COSTA, P. Photo-Fenton oxidation of phenol over a Cu-doped Fe-pillared clay. **Comptes Rendus Chimie**, v. 18, n. 10, p. 1161-1169, 2015.

HARIANI, P. L.; FATMA; RIYANTI, F.; RATNASARI, H. Adsorption of Phenol Pollutants from Aqueous Solution Using Ca-Bentonite/Chitosan Composite. **Jurnal Manusia dan Lingkungan**, v. 22, p. 233-239, 2015.

HSU, Y. C.; CHEN, Y. F.; CHEN, J. H. Decolorization of dye RB-19 solution in a continuous ozone process. **Journal of Environmental Science and Health, Part A**, v. 39, n. 1, p. 127-144, 2004.

INCHAURRONDO, N.; CONTRERAS, E.; HAURE, P. Catalyst reutilization in phenol homogeneous cupro-Fenton oxidation. **Chemical Engineering Journal**, v. 251, p. 146-157, 2014.

KAPALKA, A.; FÓTI, G.; COMNINELLIS, C. Basic principles of the electrochemical mineralization of organic pollutants for wastewater treatment. In: **Electrochemistry for the Environment**. Springer, New York, NY, p. 1-23, 2010.

KAPALKA, A.; FÓTI, G.; COMNINELLIS, C. Kinetic modelling of the electrochemical mineralization of organic pollutants for wastewater treatment. **Journal of Applied Electrochemistry**, v. 38, n. 1, p. 7-16, 2008.

KETE, M.; PLIEKHOVA, O.; MATOH, L.; ŠTANGAR, U. L. Design and evaluation of a compact photocatalytic reactor for water treatment. **Environmental Science and Pollution Research**, v. 25, n. 21, p. 20453-20465, 2018.

KITANOVIĆ, R. N.; ŠUŠTERŠIČ, V. M. Tretman otpadnih voda. **Vojnotehnički glasnik**, v. 61, n. 3, 2013.

KORNIENKO, G. V.; CHAENKO, N. V.; MAKSIMOV, N. G.; KORNIENKO, V. L.; VARNIN, V. P. Electrochemical oxidation of phenol on boron-doped diamond electrode. **Russian Journal of Electrochemistry**, v. 47, n. 2, p. 225, 2011.

LAM, F. L.; HU, X. A high performance bimetallic catalyst for photo-Fenton oxidation of Orange II over a wide pH range. **Catalysis Communications**, v. 8, n. 12, p. 2125-2129, 2007.

LI, X. Y.; CUI, Y. H.; FENG, Y. J.; XIE, Z. M.; GU, J. D. Reaction pathways and mechanisms of the electrochemical degradation of phenol on different electrodes. **Water Research**, v. 39, n. 10, p. 1972-1981, 2005.

LIU, H.; JIA, Z.; JI, S.; ZHENG, Y.; LI, M.; YANG, H. Synthesis of TiO₂/SiO₂@ Fe₃O₄ magnetic microspheres and their properties of photocatalytic degradation dyestuff. **Catalysis Today**, v. 175, n. 1, p. 293-298, 2011¹.

LIU, Z.; WANG, F.; LI, Y.; XU, T.; ZHU, S. Continuous electrochemical oxidation of methyl orange wastewater using a three-dimensional electrode reactor. **Journal of Environmental Sciences**, v. 23, p. S70-S73, 2011².

MARTÍNEZ-HUITLE, C. A.; ANDRADE, L. S. Electrocatalysis in wastewater treatment: recent mechanism advances. **Química Nova**, v. 34, p. 850-858, 2011.

MARTÍNEZ-HUITLE, C. A.; PANIZZA, M. Electrochemical oxidation of organic pollutants for wastewater treatment. **Current Opinion in Electrochemistry**, v. 11, p. 62-71, 2018.

MARTÍNEZ-HUITLE, C. A.; RODRIGO, M. A.; SIRÉS, I.; SCIALDONE, O. Single and coupled electrochemical processes and reactors for the abatement of organic water pollutants: a critical review. **Chemical Reviews**, v. 115, n. 24, p. 13362–13407, 2015.

MELO, S. A. S.; TROVÓ, A. G.; BAUTITZ, I. R.; NOGUEIRA, R. F. P. Degradação de fármacos residuais por processos oxidativos avançados. **Química Nova**, p. 188-197, 2009.

MIKLOS, D. B.; REMY, C.; JEKEL, M.; LINDEN, K. G.; DREWES, J. E.; HÜBNER, U. Evaluation of advanced oxidation processes for water and wastewater treatment – A critical review. **Water Research**, v. 139, p. 118-131, 2018.

MUANGTHAI, I.; RATANATAMSAKUL, C.; LU, M. C. Removal of 2, 4-dichlorophenol by fluidized-bed Fenton process. **Sustainable Environment Research**, v. 20, n. 5, p. 325-331, 2010.

OLIVEIRA, K. S. G. C.; VEROLI, A. B.; RUOTOLO, L. A. M. Using modulated current for energy minimization in the electrochemical treatment of effluents containing organic pollutants. **Journal of Hazardous Materials**, p. 123053, 2020.

PANIZZA, M.; CERISOLA, G. Application of diamond electrodes to electrochemical processes. **Electrochimica Acta**, v. 51, n. 2, p. 191-199, 2005.

PANIZZA, M.; KAPALKA, A.; COMNINELLIS, C. Oxidation of organic pollutants on BDD anodes using modulated current electrolysis. **Electrochimica Acta**, v. 53, n. 5, p. 2289–2295, 2008.

PELEGRINO, R. L.; DI IGLIA, R. A.; SANCHES, C. G.; AVACA, L. A.; BERTAZZOLI, R. Comparative study of commercial oxide electrodes performance in electrochemical degradation of organics in aqueous solutions. **Journal of the Brazilian Chemical Society**, v. 13, n. 1, p. 60-65, 2002.

PIMENTEL, M.; OTURAN, N.; DEZOTTI, M.; OTURAN, M. A. Phenol degradation by advanced electrochemical oxidation process electro-Fenton using a carbon felt cathode. **Applied Catalysis B: Environmental**, v. 83, n. 1-2, p. 140-149, 2008.

RADJENOVIC, J.; SEDLAK, D. L. Challenges and opportunities for electrochemical processes as next-generation technologies for the treatment of contaminated water. **Environmental Science & Technology**, v. 49, n. 19, p. 11292-11302, 2015.

RAGNINI, C. A. R. **Desenvolvimento e otimização de reatores com eletrodos tridimensionais para eletrogeração de H₂O₂**. 2001. 130 f. Tese (Doutorado em Engenharia Mecânica) - Programa de Pós-Graduação em Engenharia Mecânica, Universidade Estadual de Campinas, Campinas, 2001.

RAMÍREZ, G.; RECIO, F. J.; HERRASTI, P.; PONCE-DE-LEÓN, C.; SIRÉS, I. Effect of RVC porosity on the performance of PbO₂ composite coatings with titanate nanotubes for the electrochemical oxidation of azo dyes. **Electrochimica Acta**, v. 204, p. 9-17, 2016.

RECIO, F. J.; HERRASTI, P.; SIRÉS, I.; KULAK, A. N.; BAVYKIN, D. V.; PONCE-DE-LEON, C.; WALSH, F. C. The preparation of PbO₂ coatings on reticulated vitreous carbon for the electro-oxidation of organic pollutants. **Electrochimica Acta**, v. 56, p. 5158-5165, 2011.

RIPPEN, G. Umweltchemikalien, Ecobase Media Explorer; Verlage Chemie: Weinheim, Germany, 1998.

SALA, M.; GUTIÉRREZ-BOUZÁN, M. Carmen. Electrochemical techniques in textile processes and wastewater treatment. **International Journal of Photoenergy**, v. 2012, 2012.

SÃO PAULO. **Decreto nº 8.468, de 08 de setembro de 1976**. (Atualizado com redação dada pelo Decreto 54.487, de 26/06/09, que passa a vigorar em 180 dias após sua publicação em 27/06/09). Disponível em:

<https://www.cetesb.sp.gov.br/Institucional/documentos/Dec8468.pdf>. Acesso em: 04 nov. 2019.

SEIBERT, D.; ZORZO, C. F.; BORBA, F. H.; DE SOUZA, R. M.; QUESADA, H. B.; BERGAMASCO, R.; BAPTISTA, A. T.; INTICHER, J. J. Occurrence, statutory guideline values and removal of contaminants of emerging concern by Electrochemical Advanced Oxidation Processes: A review. **Science of The Total Environment**, p. 141527, 2020.

SOUZA, R. B. A. **Degradação eletroquímica de compostos fenólicos usando eletrodo de diamante dopado com boro**. 2012. 84 f. Dissertação (Mestrado em Engenharia Química) - Programa de Pós-Graduação em Engenharia Química, Universidade Federal de São Carlos, São Carlos, 2012.

URTIAGA, A.; GÓMEZ, P.; ARRUTI, A.; ORTIZ, I. Electrochemical removal of tetrahydrofuran from industrial wastewaters: anode selection and process scale-up. **Journal of Chemical Technology & Biotechnology**, v. 89, n. 8, p. 1243-1250, 2014.

VASCONCELOS, V. M.; PONCE-DE-LEÓN, C.; ROSIWAL, S. M.; LANZA, M. R. Electrochemical degradation of Reactive Blue 19 dye by combining boron doped diamond and reticulated vitreous carbon electrodes. **ChemElectroChem**, v. 6, n. 13, p. 3516-3524, 2019.

VEROLI, A. B. **Estudo da eletro-oxidação do paracetamol utilizando um reator eletroquímico em fluxo com eletrodo de diamante dopado com boro**. 2017. 106 f. Tese (Doutorado em Ciências) - Programa de Pós-Graduação em Química, Universidade Federal de São Carlos, São Carlos, 2017.

VILLEGAS, L. G. C.; MASHHADI, N.; CHEN, M.; MUKHERJEE, D.; TAYLOR, K. E.; BISWAS, N. A short review of techniques for phenol removal from wastewater. **Current Pollution Reports**, v. 2, n. 3, p. 157-167, 2016.

WACHTER, N. **Degradação eletroquímica do antibiótico ciprofloxacina utilizando eletrodos de diamante dopado com boro e dióxido de chumbo**. 2014. 130 f. Dissertação (Mestrado em Química) - Programa de Pós-Graduação em Química, Universidade Federal de São Carlos, São Carlos, 2014.

WANG, L.; HU, Y.; ZHANG, Y.; LI, P.; ZHAO, Y. A novel cost-saving strategy for

electrochemical oxidation of organic matters by multi-current controlled operation. **Separation and Purification Technology**, v. 109, p. 18–22, 2013.

WEISS, E.; GROENEN-SERRANO, K.; SAVALL, A. A comparison of electrochemical degradation of phenol on boron-doped diamond and lead dioxide anodes. **Journal of Applied Electrochemistry**, v. 38, n. 3, p. 329-337, 2008.

WHO. **Guidelines for drinking-water quality**: Vol. 1, Recommendations, 3 ed. World Health Organization: Geneva, 2004.

WU, D.; YANG, Z.; WANG, W.; TIAN, G.; XU, S.; SIMS, A. Ozonation as an advanced oxidant in treatment of bamboo industry wastewater. **Chemosphere**, v. 88, n. 9, p. 1108-1113, 2012.

WU, Z.; FRANKE, M.; ONDRUSCHKA, B.; ZHANG, Y.; REN, Y.; BRAEUTIGAM, P.; WANG, W. Enhanced effect of suction-cavitation on the ozonation of phenol. **Journal of hazardous materials**, v. 190, n. 1-3, p. 375-380, 2011.

YAVUZ, Y.; KOPARAL, A. S. Electrochemical oxidation of phenol in a parallel plate reactor using ruthenium mixed metal oxide electrode. **Journal of Hazardous Materials**, v. 136, n. 2, p. 296-302, 2006.

YOUSEF, R. I.; EL-ESWED, B.; ALA'A, H. Adsorption characteristics of natural zeolites as solid adsorbents for phenol removal from aqueous solutions: kinetics, mechanism, and thermodynamics studies. **Chemical Engineering Journal**, v. 171, n. 3, p. 1143-1149, 2011.

ZHU, X.; NI, J.; WEI, J.; CHEN, P. Scale-up of B-doped diamond anode system for electrochemical oxidation of phenol simulated wastewater in batch mode. **Electrochimica Acta**, v. 56, n. 25, p. 9439-9447, 2011.